

Redox-Active Tripodal Aminetris(aryloxy) Complexes of Titanium(IV)

Davide Lionetti, Andrew J. Medvecz, Vesela Ugrinova, Mauricio Quiroz-Guzman, Bruce C. Noll, and Seth N. Brown*

Department of Chemistry and Biochemistry, 251 Nieuwland Science Hall, University of Notre Dame, Notre Dame, Indiana 46556-5670

Received February 21, 2010

New sterically encumbered tripodal aminetris(aryloxy) ligands $N(CH_2C_6H_2-3-tBu-5-X-2-OH)_3$ ($tBu^X_LH_3$) with relatively electron-rich phenols are prepared by Mannich condensation ($X = OCH_3$) or by a reductive amination/Hartwig–Buchwald amination sequence on the benzyl-protected bromosalicylaldehyde ($X = N[C_6H_4-p-OCH_3]_2$), followed by debenzylation using Pearlman's catalyst ($Pd(OH)_2/C$). The analogous dianisylamino-substituted compound lacking the *tert*-butyl group *ortho* to the phenol ($H_{Ar}N_2LH_3$) is also readily prepared. The ligands are metalated by titanium(IV) *tert*-butoxide to form the five-coordinate alkoxides $LTi(O^tBu)$. Treatment of the *tert*-butoxides with aqueous HCl yields the five-coordinate chlorides $LTiCl$, and with acetylacetone gives the six-coordinate diketonates $LTi(acac)$. The diketonate complexes $tBu^X_LTi(acac)$ show reversible ligand-based oxidations with first oxidation potentials of +0.57, +0.33, and −0.09 V (vs ferrocene/ferrocenium) for $X = tBu$, MeO, and Ar_2N , respectively. Both dianisylamine-substituted complexes $R_{Ar}N_2LTi(acac)$ ($R = tBu$, H) show similar electrochemistry, with three one-electron oxidations closely spaced at ~0 V and three oxidations due to removal of a second electron from each diarylaminoaryloxy arm at ~+0.75 V. The new electron-rich tripodal ligands therefore have the capacity to release multiple electrons at unusually low potentials for aryloxy groups.

Introduction

While aryloxides have a long history as ligands to transition and main group metals, the relatively high oxidation potential of simple aryloxides means that they have only recently emerged as an important class of redox-active, “non-innocent” ligands.^{1,2} In particular, interest in the enzyme galactose oxidase, which involves a copper-coordinated tyrosyl radical,³ has spurred the preparation and characterization of copper complexes of phenoxyl radicals as spectroscopic, structural, or functional models of the enzyme.⁴ Other late-metal aroxyl complexes have also been studied.⁵ In contrast, because of the oxophilicity of d^0 transition metals and their

ability to engage in π bonding, aryloxy complexes of these metals are difficult to oxidize, and the corresponding aroxyl radical complexes have been relatively little studied. One example of such a study is that of scandium(III) complexes of sterically hindered tris(2-hydroxybenzyl)triazacyclononanes (Figure 1a), where the hexadentate, trianionic ligand confers enough stability on the oxidized complexes to observe reversible electrochemical oxidation.⁶ Titanium(IV) complexes of a similar ligand have been reported, but their oxidation was not described.⁷

*To whom correspondence should be addressed. E-mail: seth.n.brown.114@nd.edu.

(1) Chaudhuri, P.; Wieghardt, K. *Prog. Inorg. Chem.* **2001**, *50*, 151–216.

(2) The non-innocent character of catecholates, which are readily oxidized to semiquinones, has been recognized for a long time. See: Pierpont, C. G.; Lange, C. W. *Prog. Inorg. Chem.* **1994**, *41*, 331–442 and references therein.

(3) (a) Krüger, H.-J. *Angew. Chem., Int. Ed.* **1999**, *38*, 627–631. (b) Jazdzewski, B. A.; Tolman, W. B. *Coord. Chem. Rev.* **2000**, *200*, 633–685. (c) Mahadevan, V.; Klein Gebbink, R. J. M.; Stack, T. D. P. *Curr. Opin. Chem. Biol.* **2000**, *4*, 228–234.

(4) (a) Wang, Y.; DuBois, J. L.; Hedman, B.; Hodgson, K. O.; Stack, T. D. P. *Science* **1998**, *279*, 537–540. (b) Chaudhuri, P.; Hess, M.; Weyhermüller, T.; Wieghardt, K. *Angew. Chem., Int. Ed.* **1999**, *38*, 1095–1098. (c) Chaudhuri, P.; Hess, M.; Müller, J.; Hildenbrand, K.; Bill, E.; Weyhermüller, T.; Wieghardt, K. *J. Am. Chem. Soc.* **1999**, *121*, 9599–9610. (d) Rotthaus, O.; Jarjayes, O.; Thomas, F.; Philouze, C.; Saint-Aman, E.; Pierre, J.-L. *Dalton Trans.* **2007**, 889–895. (e) Mukherjee, A.; Lloret, F.; Mukherjee, R. *Inorg. Chem.* **2008**, *47*, 4471–4480. (f) Storr, T.; Verma, P.; Pratt, R. C.; Wasinger, E. C.; Shimazaki, Y.; Stack, T. D. P. *J. Am. Chem. Soc.* **2008**, *130*, 15448–15459.

(5) (a) Müller, J.; Kikuchi, A.; Bill, E.; Weyhermüller, T.; Hildebrandt, P.; Ould-Moussa, L.; Wieghardt, K. *Inorg. Chim. Acta* **2000**, *297*, 265–277. (b) Rotthaus, O.; Thomas, F.; Jarjayes, O.; Philouze, C.; Saint-Aman, E.; Pierre, J.-L. *Chem.—Eur. J.* **2006**, *12*, 6953–6962. (c) Rotthaus, O.; Jarjayes, O.; Thomas, F.; Philouze, C.; Del Valle, C. P.; Saint-Aman, E.; Pierre, J.-L. *Chem.—Eur. J.* **2006**, *12*, 2293–2302. (d) Benisvy, L.; Kannappan, R.; Song, Y.-F.; Milikisyan, S.; Huber, M.; Mutikainen, I.; Turpeinen, U.; Gamez, P.; Bernasconi, L.; Baerends, E. J.; Hartl, F.; Reedijk, J. *Eur. J. Inorg. Chem.* **2007**, 637–642. (e) Shimazaki, Y.; Kabe, R.; Huth, S.; Tani, F.; Naruta, Y.; Yamauchi, O. *Inorg. Chem.* **2007**, *46*, 6083–6090. (f) Shimazaki, Y.; Yajima, T.; Tani, F.; Karasawa, S.; Fukui, K.; Naruta, Y.; Yamauchi, O. *J. Am. Chem. Soc.* **2007**, *129*, 2559–2568. (g) Storr, T.; Wasinger, E. C.; Pratt, R. C.; Stack, T. D. P. *Angew. Chem., Int. Ed.* **2007**, *46*, 5198–5201. (h) Shimazaki, Y.; Yajima, T.; Shiraawa, T.; Yamauchi, O. *Inorg. Chim. Acta* **2009**, *362*, 2467–2474. (i) Shimazaki, Y.; Stack, T. D. P.; Storr, T. *Inorg. Chem.* **2009**, *48*, 8383–8392. (j) Rotthaus, O.; Jarjayes, O.; Philouze, C.; Del Valle, C. P.; Thomas, F. *Dalton Trans.* **2009**, 1792–1800.

(6) Adam, B.; Bill, E.; Bothe, E.; Goerd, B.; Haselhorst, G.; Hildenbrand, K.; Sokolowski, A.; Steenken, S.; Weyhermüller, T.; Wieghardt, K. *Chem.—Eur. J.* **1997**, *3*, 308–319.

(7) Auerbach, U.; Weyhermüller, T.; Wieghardt, K.; Nuber, B.; Bill, E.; Butzlaff, C.; Trautwein, A. X. *Inorg. Chem.* **1993**, *32*, 508–519.

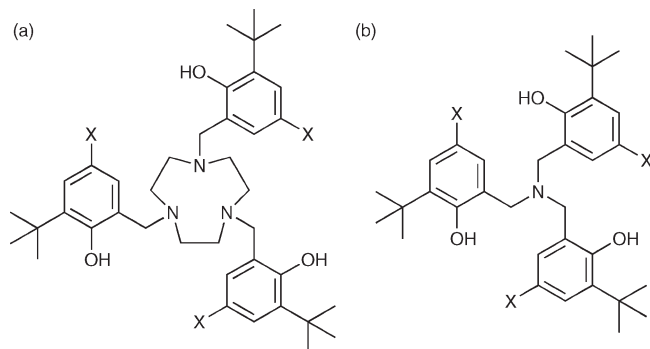


Figure 1. Chelating triphenols for investigating the redox properties of aryloxides coordinated to d^0 transition metals. (a) Hexadentate tris(3-*tert*-butyl-2-hydroxybenzyl)triazacyclononanes.⁶ (b) Tetradentate tris(3-*tert*-butyl-2-hydroxybenzyl)amines.

Another important class of chelating triaryloxide ligands are the tetradentate aminetri(aryloxides) $N(CH_2C_6H_nR_{4-n}-2-O)_3^{3-}$ (Figure 1b), which have been used extensively to form highly stable complexes with d^0 metals such as titanium(IV).⁸ In contrast to the triazacyclononane-derived ligands, the lower denticity of the aminetriphenoxides means that a metal complex may have one or two open sites available for coordination to exogenous ligands. This feature is important if one wishes to link redox events at the aryloxide ligands to stoichiometric or catalytic transformations of substrates coordinated to the metal center. Such reactions, where d^0 metal centers with redox-active ligands mediate substrate oxidation or reduction, are being explored as a new mode of metal-mediated oxidation.⁹

In addition to the coordinative properties of the metal, the electrochemical properties of the ligands are critical if redox-active ligands are to serve efficiently as electron reservoirs in multielectron transformations. The ligand must be able to store enough electrons to accomplish the desired transformation of the substrate, and must have a redox potential great enough to allow the substrate reaction to be thermodynamically favorable. For optimal energy efficiency, the overall redox potential of the ligand should be close to the thermodynamic redox potential of the substrate. In addition to having a suitable average redox potential, it should ideally also have closely spaced redox potentials for successive one-electron oxidations. Disparate redox potentials would mean that the final stages of ligand oxidation would require more energy than needed for substrate oxidation or reduction, resulting in overpotentials and concomitant energy losses.

Here we describe the redox properties of known titanium complexes of the di-*tert*-butyl-substituted tripod $N(CH_2C_6H_2-3,5-^tBu-2-O)_3^{3-}$ ($^{tBu,tBu}L^{3-}$),^{10–12} as well as those of the new, more electron-rich, methoxy-substituted tripod ligand

$N(CH_2C_6H_2-3-^tBu-5-OCH_3-2-O)_3^{3-}$ ($^{tBu,MeO}L^{3-}$). We also describe the preparation of tripodal ligands where a di-(4-methoxyphenyl)amino group (dianisylamino, An_2N) is *para* to the phenoxide oxygen, $N(CH_2C_6H_2-3-X-5-NAn_2-2-O)_3^{3-}$ ($X = H$, $^{H,An_2}N^{3-}$; $X = ^tBu$, $^{tBu,An_2}N^{3-}$). Since triarylamines are themselves redox-active and relatively electron-rich,¹³ this substituent should introduce a locus of oxidation more remote from the metal center than in unsubstituted aryloxides. If this decreases the separation between successive redox couples of the complexes, as well as lowering their average oxidation potential, it would make this novel aryloxide an attractive participant in efficient multielectron reactions.

Experimental Section

Unless otherwise noted, all procedures were carried out on the benchtop without precautions to exclude air or moisture. When dry solvents were needed, chlorinated solvents were dried over 4 Å molecular sieves, followed by CaH_2 . Benzene and toluene were dried over sodium, and ether and tetrahydrofuran over sodium benzophenone ketyl. Dry *N,N*-dimethylformamide (DMF) was anhydrous grade from Acros and was stored in the drybox until needed. Deuterated solvents were obtained from Cambridge Isotope Laboratories, dried using the same procedures as their protio analogues, and were stored in the drybox prior to use. $[N(CH_2C_6H_2-3,5-^tBu-2-O)_3]Ti(O^tBu)$ ($^{tBu,tBu}LTi[O^tBu]$),¹⁰ $^{tBu,tBu}LTi(acac)$,¹² and 5-bromo-3-*tert*-butyl-2-hydroxybenzaldehyde¹⁴ were prepared as described in the literature. All other reagents were commercially available and used without further purification. Routine NMR spectra were measured on a Varian VXR-300 spectrometer. Chemical shifts for 1H and $^{13}C\{^1H\}$ spectra are reported in parts per million (ppm) downfield of tetramethylsilane (TMS), using the known chemical shifts of the solvent residuals. Infrared spectra were recorded on NaCl plates on a Perkin-Elmer PARAGON 1000 FT-IR spectrometer. FAB mass spectra were obtained on a JEOL LMS-AX505HA mass spectrometer using the FAB ionization mode and 3-nitrobenzyl alcohol or nitrophenyl octyl ether as a matrix. Peaks reported are the mass number of the isotopomer containing all of the most abundant isotope of the constituent elements; isotope envelopes showed satisfactory agreement with calculated distributions. UV–visible spectra were measured on dichloromethane solutions (unless otherwise noted) in 1 cm quartz cuvettes using a Beckman DU-7500 diode array spectrophotometer. Elemental analyses were performed by M-H-W Laboratories (Phoenix, AZ).

Tris(3-*tert*-butyl-5-methoxy-2-hydroxybenzyl)amine, $^{tBu,MeO}LH_3$. Into a 100 mL round-bottom flask were added a stir bar, 2.42 g of hexamethylenetetramine (Aldrich, 17.2 mmol), 37.17 g of 2-*tert*-butyl-4-methoxyphenol (Aldrich, 206.2 mmol), and 6.2 mL of 37% aqueous formaldehyde (83 mmol). The flask was fitted with a reflux condenser and a heating mantle, and was heated to reflux. After 3 d, reflux was stopped, and the reaction mixture was allowed to cool to room temperature. The mixture was dissolved in 200 mL of $CHCl_3$ and transferred to a 1000 mL beaker. To the mixture was added 200 mL of 1 M hydrochloric acid and a magnetic stir bar. After several minutes of stirring, a white precipitate formed. The aqueous layer was decanted off, and the organic layer was filtered on a glass frit and the solid washed with 2×20 mL of chloroform. The solid was transferred to a 1 L Erlenmeyer flask, and 400 mL of CH_2Cl_2 and 500 mL of saturated aqueous sodium bicarbonate solution were added. The mixture was stirred overnight to dissolve all the solid. The

(8) Licini, G.; Mba, M.; Zonta, C. *Dalton Trans.* **2009**, 5265–5277.

(9) (a) Haneline, M. R.; Heyduk, A. F. *J. Am. Chem. Soc.* **2006**, *128*, 8410–8411. (b) Stanciu, C.; Jones, M. E.; Fanwick, P. E.; Abu-Omar, M. M. *J. Am. Chem. Soc.* **2007**, *129*, 12400–12401. (c) Zarkesh, R. A.; Ziller, J. W.; Heyduk, A. F. *Angew. Chem., Int. Ed.* **2008**, *47*, 4715–4718. (d) Blackmore, K. J.; Lal, N.; Ziller, J. W.; Heyduk, A. F. *J. Am. Chem. Soc.* **2008**, *130*, 2728–2729. (e) Nguyen, A. I.; Blackmore, K. J.; Carter, S. M.; Zarkesh, R. A.; Heyduk, A. F. *J. Am. Chem. Soc.* **2009**, *131*, 3307–3316.

(10) Kol, M.; Shamis, M.; Goldberg, I.; Goldschmit, Z.; Alf, S.; Hayut-Salant, E. *Inorg. Chem. Commun.* **2001**, *4*, 177–179.

(11) Ugrinova, V.; Ellis, G. A.; Brown, S. N. *Chem. Commun.* **2004**, 468–469.

(12) Fortner, K. C.; Bigi, J. P.; Brown, S. N. *Inorg. Chem.* **2005**, *44*, 2803–2814.

(13) Amthor, S.; Noller, B.; Lambert, C. *Chem. Phys.* **2005**, *316*, 141–152.

(14) Cavazzini, M.; Manfredi, A.; Montanari, F.; Quici, S.; Pozzi, G. *Eur. J. Org. Chem.* **2001**, 4639–4649.

organic layer was collected, dried over magnesium sulfate, filtered, and the solvent evaporated on a rotary evaporator to obtain a light yellow oil. The oil was dissolved in methanol (100 mL), and the solution allowed to stand for 3 d at room temperature, at which point large colorless blocks had precipitated. The solid was filtered, washed with methanol, and air-dried on a glass frit to yield 4.19 g of $t\text{-Bu}_2\text{MeO}^-\text{LH}_3$ (10%). ^1H NMR (CDCl_3): δ 1.37 (s, 27H, $\text{ArC}(\text{CH}_3)_3$), 3.61 (s, 6H, NCH_2Ar), 3.75 (s, 9H, OCH_3), 6.54 (d, 3 Hz, 3H, ArH), 6.83 (d, 3 Hz, 3H, ArH). $^{13}\text{C}\{^1\text{H}\}$ NMR (CDCl_3): δ 29.71, 35.15, 55.87, 56.72, 113.32, 114.13, 123.33, 139.30, 147.90, 152.85. IR (evaporated film, cm^{-1}): 3542 (s, br, ν_{OH}), 2999 (m), 2954 (s), 2906 (s), 2835 (m), 1605 (s), 1476 (s), 1456 (s), 1434 (s), 1392 (m), 1361 (m), 1311 (m), 1270 (m), 1213 (s), 1134 (m), 1094 (m), 1059 (s), 1024 (w), 1001 (w), 978 (w), 945 (w), 916 (w), 854 (m), 800 (m), 770 (m), 755 (m), 735 (m), 704 (w), 690 (w). FAB-MS: 593 (M^+). Anal. Calcd for $\text{C}_{36}\text{H}_{51}\text{NO}_6$: C, 72.82; H, 8.66; N, 2.36. Found: C, 72.51; H, 8.34; N, 2.46.

2-Benzyloxy-5-bromobenzaldehyde. In a 100 mL round-bottom flask were placed 5.00 g of 5-bromosalicylaldehyde (Alfa Aesar, 24.9 mmol), 13.12 g of potassium carbonate (95.0 mmol, 3.8 equiv), and a magnetic stirbar. The flask was filled with nitrogen and capped with a septum, and 23 mL of dry DMF were added, followed by 5.08 g of benzyl bromide (29.7 mmol, 1.2 equiv) dissolved in 10 mL of dry DMF. After stirring 18 h, the reaction mixture was poured into 107 mL of distilled water, forming a light yellow precipitate. The solution was filtered on a glass frit, and the solid washed with H_2O to obtain 7.19 g of 2-benzyloxy-5-bromobenzaldehyde (99%). Spectroscopic data were in agreement with published values.¹⁵

Tris(2-benzyloxy-5-bromobenzyl)amine, $\text{N}(\text{CH}_2\text{C}_6\text{H}_3\text{-5-Br-2-OCH}_2\text{Ph})_3$. In the drybox, ammonium acetate (0.359 g, 4.66 mmol), 2-benzyloxy-5-bromobenzaldehyde (4.07 g, 13.98 mmol, 3.0 equiv), and sodium triacetoxyborohydride (4.44 g, 21.0 mmol, 4.5 equiv) were placed into a 50 mL round-bottom flask. A stirbar and dry tetrahydrofuran (THF) were added, and the flask was stoppered with a rubber septum. After stirring for 22 h, the volatiles were removed on a rotary evaporator. The oily residue was dissolved in ethyl acetate, and the resulting solution was washed with 2×35 mL of 5% aqueous KOH and 35 mL of brine. The organic layer was collected, dried over magnesium sulfate, and evaporated to dryness to yield a light yellow oil which solidified into a white solid. The solid was washed with methanol and air-dried on a glass frit to obtain 2.19 g of tris(2-benzyloxy-5-bromobenzyl)amine (26.0 mmol, 56%). ^1H NMR (CDCl_3): δ 3.73 (s, 6H, NCH_2Ar), 5.05 (s, 6H, OCH_2Ph), 6.69 (d, 9 Hz, 3H, Ar 3-H), 7.20 (dd, 9 Hz, 2.5 Hz, 3H, Ar 4-H), 7.34 (m, 15H, $\text{OCH}_2\text{C}_6\text{H}_5$), 7.65 (d, 2.5 Hz, 3H, Ar 6-H). $^{13}\text{C}\{^1\text{H}\}$ NMR (CDCl_3): δ 52.77 (NCH_2), 70.39 (OCH_2Ph), 113.35, 113.57, 127.26, 128.05, 128.81, 130.54, 130.62, 132.92, 137.11, 155.97. IR (evapd film, cm^{-1}): 3093 (w), 3065 (w), 3032 (w), 2926 (w), 2867 (w), 1591 (m), 1485 (s), 1454 (s), 1403 (m), 1371 (m), 1240 (s), 1179 (m), 1135 (m), 1105 (m), 1025 (m), 970 (w), 890 (w), 848 (w), 802 (m), 735 (s), 696 (s), 652 (m). FAB-MS: 840 ($\text{M}^+ + \text{H}$, $^{79}\text{Br}_3$ isotopomer). Anal. Calcd for $\text{C}_{42}\text{H}_{36}\text{Br}_3\text{NO}_3$: C, 59.88; H, 4.31; 1.66. Found: C, 60.16; H, 4.54; N, 1.67.

Tris(2-benzyloxy-5-[(di-*p*-methoxyphenyl)amino]benzyl)amine, $\text{N}(\text{CH}_2\text{C}_6\text{H}_3\text{-5-[N(C}_6\text{H}_4\text{OCH}_3)_2\text{-2-OCH}_2\text{Ph}]})_3$. In the drybox, tris(2-benzyloxy-5-bromobenzyl)amine (2.19 g, 2.60 mmol) was dissolved in 7 mL of dry benzene. Into a 20 mL screw-cap scintillation vial were added 1.79 g of 4,4'-dimethoxydiphenylamine (Alfa Aesar, 7.81 mmol, 3.0 equiv), 1.13 g of sodium *tert*-butoxide (Aldrich, 11.8 mmol, 4.5 equiv), 80.0 mg of tris(dibenzylideneacetone)dipalladium (Strem, 0.0874 mmol, 2.2 mol % Pd per Br), and a stirbar. The tris(2-benzyloxy-5-bromobenzyl)amine solution was added to the solid reagents in the vial, followed by a

solution of 28.0 mg of tri-*tert*-butylphosphine (Strem, 0.138 mmol, 1.8 mol % per Br) in 2 mL of benzene. The vial was then capped tightly and taken out of the drybox. After 17 h stirring at room temperature, the vial was opened to the air and the reaction mixture poured into a 50 mL round-bottom flask containing 15 mL of saturated aqueous ammonium chloride. The reaction vial was rinsed with a few milliliters of ether, and the washing combined with the rest of the mixture. The aqueous/organic mixture was stirred for 5 min and then transferred to a separatory funnel. The organic layer was collected, dried over magnesium sulfate, filtered, and evaporated to dryness to obtain 3.17 g of a dark brown oil (95%). ^1H NMR (CDCl_3): δ 3.64 (s, 18H, OCH_3), 3.68 (s, 6H, NCH_2Ar), 4.88 (s, 6H, OCH_2Ph), 6.61 (d, 9 Hz, 12H, 2,6- $\text{NC}_6\text{H}_4\text{OCH}_3$), 6.65 (br m, 6H, Ar 4-H , 6-H), 6.81 (d, 9 Hz, 12H, 3,5- $\text{NC}_6\text{H}_4\text{OCH}_3$), 7.12 (br m, 3H, Ar 3-H), 7.31 (m, 15H, $\text{OCH}_2\text{C}_6\text{H}_5$). $^{13}\text{C}\{^1\text{H}\}$ NMR: δ 53.16 (NCH_2), 55.53 (OCH_3), 70.21 (OCH_2Ph), 112.23, 114.43, 122.64, 124.46, 125.25, 127.28, 127.74, 128.64, 129.40, 137.92, 141.75, 142.17, 152.33, 154.62. IR (evapd film, cm^{-1}): 3041 (w), 2999 (w), 2947 (w), 2906 (w), 2833 (w), 1605 (w), 1588 (w), 1503 (s), 1463 (m), 1372 (w), 1280 (w), 1238 (s), 1180 (w), 1106 (w), 1037 (m), 917 (w), 825 (w), 736 (w), 697 (w). FAB MS: 1287 ($\text{M}^+ + \text{H}$). Anal. Calcd for $\text{C}_{84}\text{H}_{78}\text{N}_4\text{O}_9$: C, 78.35; H, 6.11; N, 4.35. Found: C, 78.41; H, 6.16; N, 4.24.

Tris(2-hydroxy-5-[(di-*p*-methoxyphenyl)amino]benzyl)amine, $\text{H}_3\text{A}_{\text{N}_2}\text{N}^-\text{LH}_3$. To a solution of the benzyl-protected ligand $\text{N}(\text{CH}_2\text{C}_6\text{H}_3\text{-5-[N(C}_6\text{H}_4\text{OCH}_3)_2\text{-2-OCH}_2\text{Ph}]})_3$ (3.07 g, 2.39 mmol) in 20 mL of EtOAc were added 0.31 g of palladium, 10 wt % on activated carbon (Aldrich). The flask was flushed with hydrogen and stirred 5 d under balloon pressure of H_2 . The mixture was gravity filtered, and the solvent evaporated from the filtrate to obtain a dark brown oil. Trituration with methanol/water gave a light brown precipitate, which was isolated by suction filtration and dried under vacuum overnight to obtain 2.23 g (92%) of $\text{N}(\text{CH}_2\text{C}_6\text{H}_3\text{-5-[N(C}_6\text{H}_4\text{OCH}_3)_2\text{-2-OH}]})_3$, $\text{H}_3\text{A}_{\text{N}_2}\text{N}^-\text{LH}_3$. ^1H NMR (CDCl_3): δ 3.62 (br s, 6H, NCH_2Ar), 3.75 (s, 18H, OCH_3), 6.75 (m, 21H, $\text{ArH} + 2,6\text{-NC}_6\text{H}_4\text{OCH}_3$), 6.94 (br d, 9 Hz, 12H, 3,5- $\text{NC}_6\text{H}_4\text{OCH}_3$), 7.46 (v br s, 3H, OH). $^{13}\text{C}\{^1\text{H}\}$ NMR (CDCl_3): δ 55.68 (NCH_2), 57.23 (OCH_3), 114.69, 117.25, 119.75, 123.25, 124.91, 126.35, 141.25, 142.14, 151.31, 155.02. IR (evapd film, cm^{-1}): 3310 (w, br, ν_{OH}), 2998 (w), 2926 (w), 2849 (w), 2906 (w), 2833 (w), 1662 (w), 1606 (w), 1586 (w), 1504 (s), 1464 (m), 1440 (m), 1322 (w), 1239 (s), 1178 (m), 1107 (w), 1036 (m), 953 (w), 877 (w), 826 (m), 779 (w), 718 (w), 580 (w). FAB-MS: 1017 ($\text{M} + \text{H}$)⁺. Anal. Calcd for $\text{C}_{63}\text{H}_{60}\text{N}_4\text{O}_9$: C, 74.39; H, 5.95; N, 5.51. Found: C, 74.67; H, 6.17; N, 5.31.

2-Benzyloxy-3-*tert*-butyl-5-bromobenzaldehyde. 5-Bromo-3-*tert*-butyl-2-hydroxybenzaldehyde (11.22 g, 43.6 mmol) was benzylated in DMF (40 mL) using PhCH_2Br (8.95 g, 52.3 mmol, 1.2 equiv, dissolved in 30 mL of DMF) and K_2CO_3 (22.91 g, 64.9 mmol, 3.8 equiv) as described above for 5-bromo-2-hydroxybenzaldehyde. After quenching the reaction with water (300 mL), the mixture was extracted with 100 mL of hexane. The organic layer was collected, dried over magnesium sulfate, and the solvent evaporated to give a yellow oil. Purification by column chromatography on silica gel (15:1 hexanes/ether) yielded 10.83 g (71%) of the benzylated bromosalicylaldehyde as a pale yellow solid. ^1H NMR (CDCl_3): δ 1.44 (s, 9H, $\text{C}(\text{CH}_3)_3$), 5.04 (s, 2H, OCH_2Ph), 7.49 (m, 5H, $\text{OCH}_2\text{C}_6\text{H}_5$), 7.70 (d, 2.4 Hz, 1H, ArH), 7.85 (d, 2.4 Hz, 1H, ArH). $^{13}\text{C}\{^1\text{H}\}$ NMR (CDCl_3): δ 30.89 ($\text{C}(\text{CH}_3)_3$), 35.69 ($\text{C}(\text{CH}_3)_3$), 81.05 (OCH_2), 117.82 (CBr), 127.26, 128.64, 128.98, 130.31, 131.61, 136.10, 136.58, 146.82, 161.07 (COCH_2Ph), 189.06 (CHO). IR (evapd film, cm^{-1}): 3093 (w), 3061 (w), 3030 (w), 2963 (w), 2916 (w), 2871 (w), 2740 (w), 1689 (s, $\nu_{\text{C=O}}$), 1607 (w), 1569 (m), 1498 (w), 1455 (m), 1433 (s), 1370 (s), 1332 (w), 1311 (w), 1236 (s), 1206 (s), 1156 (s), 1104 (w), 1078 (w), 1000 (m), 969 (m), 918 (w), 882 (m), 865 (w), 842 (w), 803 (m), 765 (w), 735 (m), 696 (m), 661

(15) Fresneda, P. M.; Molina, P.; Bleda, J. A. *Tetrahedron* **2001**, *57*, 2355–2363.

(m). FAB MS: 346 (M^+ , ^{79}Br isotopomer). Anal. Calcd for $\text{C}_{18}\text{H}_{19}\text{BrO}_2$: C, 62.26; H, 5.51. Found: C, 62.68; H, 5.11.

Tris(2-benzyloxy-3-*tert*-butyl-5-bromobenzyl)amine. In a 50 mL round-bottom flask in the drybox were combined 0.95 g of ammonium acetate (12.3 mmol), 12.83 g of 2-benzyloxy-5-bromo-3-*tert*-butylbenzaldehyde (36.96 mmol, 3.0 equiv), and 11.75 g of sodium triacetoxymethylborohydride (55.44 mmol, 4.5 equiv). A stirbar was added, and the flask sealed with a Teflon needle valve. Dry 1,2-dichloroethane (100 mL) was added to the reaction flask by vacuum transfer, and the reaction mixture was stirred for 3 d. The volatiles were removed on a rotary evaporator, and the residue was dissolved in EtOAc (2×100 mL). The solution was washed with 2×50 mL of 5% aqueous KOH solution and 50 mL of brine. The organic layer was collected, dried over magnesium sulfate, and the solvent was evaporated to obtain the crude product as a light yellow oil. After standing 2 d at room temperature, the mixture deposited clear crystals which were washed with hexane. The hexane supernatant was then evaporated and purified by column chromatography on silica gel, eluting with 5% ethyl acetate in hexanes to give a light yellow solid that was recrystallized from hot hexanes. The combined products yielded 7.31 g of tris(2-benzyloxy-5-bromo-3-*tert*-butylbenzyl)amine (59%) as a colorless solid. ^1H NMR (CDCl_3): δ 1.34 (s, 27H, $\text{C}(\text{CH}_3)_3$), 3.57 (s, 6H, NCH_2), 4.69 (s, 6H, OCH_2Ph), 7.30 (m, 15H, $\text{OCH}_2\text{C}_6\text{H}_5$), 7.34 (d, 2.4 Hz, 3H, *ArH*), 7.59 (d, 2.4 Hz, 3H, *ArH*). $^{13}\text{C}\{^1\text{H}\}$ NMR (CDCl_3): δ 31.06 ($\text{C}(\text{CH}_3)_3$), 35.57 ($\text{C}(\text{CH}_3)_3$), 52.00 (NCH_2), 75.93 (OCH_2), 117.46 (CBr), 126.88, 127.84, 128.70, 129.65, 131.59, 134.84, 137.17, 145.41, 156.29. IR (evapd film, cm^{-1}): 2962 (s), 2909 (m), 2876 (m), 1570 (w), 1498 (w), 1454 (m), 1430 (s), 1404 (w), 1367 (s), 1263 (w), 1211 (s), 1156 (s), 1106 (w), 1014 (w), 979 (m), 871 (w), 843 (w), 733 (m), 694 (m). FAB MS: 1007 (M^+ , $^{79}\text{Br}_3$ isotopomer). Anal. Calcd for $\text{C}_{54}\text{H}_{60}\text{Br}_3\text{NO}_3$: C, 64.17; H, 5.98; N, 1.39. Found: C, 64.09; H, 6.18; N, 1.47.

Tris(2-benzyloxy-3-*tert*-butyl-5-[(*di-p*-methoxyphenyl)amino]benzyl)amine. Tris(2-benzyloxy-3-*tert*-butyl-5-bromobenzyl)amine (7.31 g, 7.23 mmol) was aminated with 4,4'-dimethoxydiphenylamine (4.97 g, 21.7 mmol, 3 equiv) as described above for tris(2-benzyloxy-5-bromobenzyl)amine, except that the reaction was allowed to stir for 3 d. The crude material was purified by recrystallization from 2:1 hexanes/ether at -20°C , yielding a yellow crystalline solid. Three crops gave a total yield of 9.32 g (88%). This compound is slightly sensitive to air and light and was stored wrapped in foil in the drybox. ^1H NMR (CDCl_3): δ 1.22 (s, 27H, $\text{C}(\text{CH}_3)_3$), 3.58 (s, 6H, NCH_2), 3.66 (s, 18H, OCH_3), 4.67 (s, 6H, OCH_2Ph), 6.64 (d, 9 Hz, 12H, $\text{NC}_6\text{H}_4\text{OCH}_3$ 2,6-H), 6.81 (d, 2.5 Hz, 3H, *ArH*), 6.82 (d, 9 Hz, 12H, $\text{NC}_6\text{H}_4\text{OCH}_3$ 3,5-H), 6.97 (d, 2.5 Hz, 3H, *ArH*), 7.22 (m, 15H, $\text{OCH}_2\text{C}_6\text{H}_5$). $^{13}\text{C}\{^1\text{H}\}$ NMR (CDCl_3): δ 31.39 ($\text{C}(\text{CH}_3)_3$), 35.46 ($\text{C}(\text{CH}_3)_3$), 52.77 (NCH_2), 55.65 (OCH_3), 75.33 ($\text{OCH}_2\text{-Ph}$), 114.62, 121.41, 123.09, 125.18, 127.16, 127.57, 128.60, 133.45, 138.06, 142.02, 143.47, 143.81, 151.85, 155.01. IR (evapd film, cm^{-1}): 3036 (s), 2999 (s), 2955 (s), 2834 (s), 1681 (w), 1654 (w), 1595 (s), 1510 (s), 1463 (s), 1441 (s), 1391 (w), 1370 (s), 1328 (m), 1296 (m), 1242 (s), 1209 (s), 1180 (m), 1135 (w), 1106 (m), 1078 (w), 1038 (s), 1017 (m), 927 (w), 914 (w), 873 (w), 862 (w), 827 (s), 792 (w), 780 (m), 764 (m), 736 (s), 699 (s), 640 (m), 601 (s). FAB MS: 1455 (M^+ + H). Anal. Calcd for $\text{C}_{96}\text{H}_{102}\text{N}_4\text{O}_9$: C, 79.20; H, 7.06; N, 3.85. Found: C, 79.40; H, 7.02; N, 3.59.

Tris(2-hydroxy-3-*tert*-butyl-5-[(*di-p*-methoxyphenyl)amino]benzyl)amine, $^t\text{Bu}_3\text{ALi}^+\text{LH}_3^-$. In a 250 mL round-bottom flask, 9.32 g of tris(2-benzyloxy-3-*tert*-butyl-5-[(*di-p*-methoxyphenyl)amino]benzyl)amine (6.40 mmol) was dissolved in 100 mL of EtOAc. Pearlman's catalyst ($\text{Pd}(\text{OH})_2$, 20% on activated carbon, wet [50% water], 3.73 g, 40% loading by mass) was added to the solution. The flask was flushed with hydrogen, and the reaction mixture was stirred for 5 d under a hydrogen-filled balloon. The catalyst was removed from the reaction mixture by

gravity filtration, and the solvent was evaporated to yield a crude brown oil. The oil was dissolved in 30 mL of CH_2Cl_2 and washed with 100 mL of 0.01 M aqueous sodium dithionite to give a clear, yellow solution. The biphasic mixture was allowed to stir under nitrogen for 30 min. The organic layer was dried over MgSO_4 under N_2 , then filtered under N_2 to give a yellow solution. The solvent was removed in vacuo to give a pale yellow solid, which was isolated and stored in the drybox (5.59 g, 73%). ^1H NMR (CDCl_3): δ 1.31 (s, 27H, $\text{C}(\text{CH}_3)_3$), 3.45 (s, 6H, NCH_2), 3.77 (s, 18H, OCH_3), 6.27 (br s, 3H, *OH*), 6.60 (d, 2.5 Hz, 3H, *ArH*), 6.75 (d, 9 Hz, 12H, $\text{NC}_6\text{H}_4\text{OCH}_3$ 2,6-H), 6.94 (d, 9 Hz, 12H, $\text{NC}_6\text{H}_4\text{OCH}_3$ 3,5-H), 6.97 (d, 2.5 Hz, 3H, *ArH*). $^{13}\text{C}\{^1\text{H}\}$ NMR (CDCl_3): 29.77 ($\text{C}(\text{CH}_3)_3$), 35.04 ($\text{C}(\text{CH}_3)_3$), 55.64 (NCH_2), 56.26 (OCH_3), 114.66, 123.27, 123.38, 124.12, 124.91, 138.64, 141.07, 142.14, 149.20, 154.99. IR (nujol mull, cm^{-1}): 2951 (m), 2852 (m), 1603 (w), 1502 (m), 1364 (w), 1332 (w), 1297 (w), 1270 (w), 1237 (m), 1178 (w), 1134 (w), 1105 (w), 1035 (w), 1009 (w), 872 (w), 856 (w), 824 (w), 793 (w), 770 (w), 724 (w). FAB-MS: 1185 (M^+). Anal. Calcd for $\text{C}_{75}\text{H}_{84}\text{N}_4\text{O}_9$: C, 75.99; H, 7.14; N, 4.73. Found: C, 75.60; H, 7.30; N, 4.71.

$^t\text{Bu}_3\text{MeO}^+\text{Li}^+(\text{O}^t\text{Bu})^-$. In the drybox, 0.807 g of $^t\text{Bu}_3\text{MeO}^+\text{Li}^+(\text{O}^t\text{Bu})^-$ (1.36 mmol) and 0.464 g of titanium *tert*-butoxide (Strem, 1.36 mmol) were dissolved in 30 mL of CH_2Cl_2 in a 100 mL round-bottom flask. The reaction was stirred for 5 min under N_2 . Evaporation of the solvent on the rotary evaporator yielded 0.963 g (99%) of bright yellow air-stable $^t\text{Bu}_3\text{MeO}^+\text{Li}^+(\text{O}^t\text{Bu})^-$. ^1H NMR (CDCl_3): δ 1.45 (s, 27H, $\text{ArC}(\text{CH}_3)_3$), 1.63 (s, 9H, $\text{OC}(\text{CH}_3)_3$), 2.84 (d, 14 Hz, 3H, CHH'), 3.74 (s, 9H, OCH_3), 3.95 (d, 14 Hz, 3H, CHH'), 6.50 (d, 3 Hz, 3H, *ArH*), 6.77 (d, 3 Hz, 3H, *ArH*). $^{13}\text{C}\{^1\text{H}\}$ NMR (CDCl_3): δ 29.72 ($\text{ArC}(\text{CH}_3)_3$), 32.62 ($\text{OC}(\text{CH}_3)_3$), 35.34 ($\text{ArC}(\text{CH}_3)_3$), 55.88 (NCH_2), 58.76 (OCH_3), 85.76 ($\text{OC}(\text{CH}_3)_3$), 111.80, 112.63, 125.50, 137.55, 152.66, 157.50. IR (evapd film, cm^{-1}): 2951 (m), 1602 (w), 1464 (s), 1429 (s), 1358 (w), 1325 (w), 1235 (s), 1208 (s), 1178 (m), 1060 (m), 1024 (s), 921 (w), 848 (s), 795 (w), 762 (w). FAB-MS: 711 (M^+). Anal. Calcd for $\text{C}_{40}\text{H}_{57}\text{NO}_7\text{Ti}$: C, 67.50; H, 8.07; N, 1.97. Found: C, 66.05; H, 7.36; N, 2.00.

$^t\text{Bu}_3\text{An}_2\text{N}^+\text{Li}^+(\text{O}^t\text{Bu})^-$. The compound was prepared analogously using 0.4202 g of $^t\text{Bu}_3\text{An}_2\text{N}^+\text{Li}^+(\text{O}^t\text{Bu})^-$ (0.3544 mmol) and 0.1246 g of titanium *tert*-butoxide (0.3624 mmol) to yield 0.4656 g (99%) of orange $^t\text{Bu}_3\text{An}_2\text{N}^+\text{Li}^+(\text{O}^t\text{Bu})^-$, which is stable for brief periods in the air but should be stored in the drybox. ^1H NMR (CDCl_3): δ 1.38 (s, 27H, $\text{ArC}(\text{CH}_3)_3$), 1.64 (s, 9H, $\text{OC}(\text{CH}_3)_3$), 2.63 (d, 13 Hz, 3H, CHH'), 3.77 (s, 18H, OCH_3), 3.92 (d, 14 Hz, 3H, CHH'), 6.55 (d, 2.5 Hz, 3H, *ArH*), 6.75 (d, 9 Hz, 12H, $\text{NC}_6\text{H}_4\text{OCH}_3$ 2,6-H), 6.90 (d, 9 Hz, 12H, $\text{NC}_6\text{H}_4\text{OCH}_3$ 3,5-H), 6.93 (d, 2 Hz, 3H, *ArH*). $^{13}\text{C}\{^1\text{H}\}$ NMR (CDCl_3): δ 29.88 ($\text{ArC}(\text{CH}_3)_3$), 32.59 ($\text{OC}(\text{CH}_3)_3$), 35.22 ($\text{ArC}(\text{CH}_3)_3$), 55.69 (OCH_3), 58.49 (NCH_2), 77.43 ($\text{OC}(\text{CH}_3)_3$), 114.64, 121.69, 122.47, 125.05, 125.76, 136.95, 140.87, 142.18, 155.02, 158.89. IR (evapd film, cm^{-1}): 2953 (m), 2833 (w), 1599 (m), 1505 (s), 1463 (m), 1441 (m), 1389 (w), 1359 (w), 1335 (w), 1297 (w), 1240 (s), 1180 (m), 1144 (w), 1106 (w), 1037 (m), 1021 (m), 882 (m), 828 (m), 819 (m), 739 (m), 686 (w), 637 (w), 599 (w). Anal. Calcd for $\text{C}_{79}\text{H}_{90}\text{N}_4\text{O}_{10}\text{Ti}$: C, 72.80; H, 6.96; N, 4.30. Found: C, 72.65; H, 7.01; N, 4.08.

$^t\text{Bu}_3\text{Bu}^+\text{Li}^+(\text{O}^t\text{Bu})^-$. A yellow solution of $^t\text{Bu}_3\text{Bu}^+\text{Li}^+(\text{O}^t\text{Bu})^-$ (0.5000 g, 0.665 mmol) in 20 mL of C_6H_6 was placed in a 125 mL separatory funnel and shaken with 50 mL of 1 M HCl for 10 min. The red C_6H_6 layer was collected and dried over MgSO_4 , and the solvent was removed on a rotary evaporator to give 0.4551 g of red $^t\text{Bu}_3\text{Bu}^+\text{Li}^+(\text{O}^t\text{Bu})^-$ (91%). ^1H NMR (CDCl_3): δ 1.28 (s, 27H, $\text{C}(\text{CH}_3)_3$), 1.45 (s, 27H, $\text{C}(\text{CH}_3)_3$), 3.09 (d, 14 Hz, 3H, CHH'), 4.07 (d, 14 Hz, 3H, CHH'), 7.02 (d, 2 Hz, 3H, *ArH*), 7.25 (d, 2 Hz, 3H, *ArH*). $^{13}\text{C}\{^1\text{H}\}$ NMR (CDCl_3): δ 29.77 ($\text{C}(\text{CH}_3)_3$), 31.79 ($\text{C}(\text{CH}_3)_3$), 34.70 ($\text{C}(\text{CH}_3)_3$), 35.13 ($\text{C}(\text{CH}_3)_3$), 58.99 (NCH_2), 123.53, 123.76, 124.16, 135.98, 144.51, 161.06. EI MS: 751 (M^+). IR (evapd film, cm^{-1}): 3091 (w), 3034 (w), 2959 (s), 2906 (s), 2869 (s), 1773 (w), 1601 (m), 1476 (s), 1446 (s),

1414 (m), 1393 (m), 1362 (s), 1306 (m), 1290 (m), 1254 (s), 1238 (s), 1204 (s), 1171 (s), 1127 (s), 1071 (m), 1028 (w), 981 (w), 962 (w), 918 (s), 866 (s), 814 (m), 764 (s), 740 (m), 693 (m), 677 (m), 650 (m), 609 (s), 590 (m), 570 (w). Anal. Calcd for $C_{45}H_{66}ClNO_3Ti$: C, 71.84; H, 8.84; N, 1.86. Found: C, 72.03; H, 8.69; N, 1.82.

tBu,MeO LTiCl. The compound was prepared from tBu,MeO LTi(O'Bu) (0.373 g, 0.523 mmol) by the same procedure to give 0.334 g of tBu,MeO LTiCl (95%). 1H NMR ($CDCl_3$): δ 1.44 (s, 27H, $C(CH_3)_3$), 3.04 (br d, 14 Hz, 3H, CHH'), 3.76 (s, 9H, OCH_3), 4.03 (br d, 14 Hz, 3H, CHH'), 6.55 (d, 3 Hz, 3H, ArH), 6.81 (d, 3 Hz, 3H, ArH). $^{13}C\{^1H\}$ NMR ($CDCl_3$): δ 29.57 ($C(CH_3)_3$), 35.15 ($C(CH_3)_3$), 55.84 (OCH_3), 58.63 (NCH_2), 111.78, 112.90, 124.64, 138.40, 153.99, 157.84. IR (evapd film, cm^{-1}): 2993 (w), 2956 (s), 2906 (m), 2869 (m), 2835 (w), 1601 (s), 1467 (s), 1431 (s), 1392 (w), 1360 (w), 1327 (m), 1288 (w), 1231 (s), 1208 (s), 1177 (w), 1143 (m), 1058 (s), 1025 (w), 984 (w), 920 (m), 865 (s), 797 (w), 756 (w). FAB-MS: 673 (M^+). Anal. Calcd for $C_{36}H_{48}ClNO_6Ti$: C, 64.14; H, 7.18; N, 2.08. Found: C, 63.94; H, 6.93; N, 2.20.

tBu,An_2N LTiCl. The compound was prepared from tBu,An_2N LTi(O'Bu) (0.2094 g, 0.1607 mmol) by the same procedure to give 0.1518 g of tBu,An_2N LTiCl (75%). 1H NMR ($CDCl_3$): δ 1.26 (s, 27H, $C(CH_3)_3$), 2.67 (d, 14 Hz, 3H, CHH'), 3.68 (s, 18H, OCH_3), 3.90 (d, 13 Hz, 3H, CHH'), 6.43 (d, 2.5 Hz, 3H, ArH), 6.68 (d, 9 Hz, 12H, $NC_6H_4OCH_3$ 2,6-H), 6.80 (d, 2.5 Hz, 3H, ArH), 6.85 (d, 9 Hz, 12H, $NC_6H_4OCH_3$ 3,5-H). $^{13}C\{^1H\}$ NMR ($CDCl_3$): δ 29.71 ($C(CH_3)_3$), 35.07 ($C(CH_3)_3$), 55.68 (OCH_3), 58.47 (NCH_2), 114.79, 120.69, 120.88, 124.78, 125.76, 137.68, 141.65, 142.75, 155.52, 158.80. IR (evapd film, cm^{-1}): 2998 (w), 2956 (m), 2908 (w), 2870 (w), 2834 (w), 2068 (w), 1638 (m), 1597 (m), 1507 (s), 1464 (m), 1441 (m), 1392 (w), 1359 (w), 1336 (w), 1298 (w), 1240 (s), 1217 (m), 1181 (w), 1168 (w), 1143 (w), 1105 (w), 1038 (m), 866 (w), 892 (m), 828 (m), 818 (m), 781 (w), 746 (m), 712 (w), 607 (w). Anal. Calcd for $C_{75}H_{81}ClN_4O_6Ti$: C, 71.17; H, 6.45; N, 4.43. Found: C, 71.31; H, 6.65; N, 4.34.

tBu,tBu LTi(acac) was prepared as described previously.¹² UV-vis (CH_2Cl_2) λ_{max} 259 nm ($\epsilon = 34000 M^{-1} cm^{-1}$), 340 (sh, 12000), 366 (12900).

tBu,MeO LTi(acac). A solution of 0.300 g of tBu,MeO LTi(O'Bu) (0.421 mmol) in 15 mL of CH_2Cl_2 was treated with 0.041 mL of 2,4-pentanedione (0.42 mmol, 1.0 equiv) and stirred for 2 h. Evaporation of the solvent yielded 0.296 g of tBu,MeO LTi(acac) as a dark orange solid (95%). 1H NMR ($CDCl_3$): δ 1.30 (s, 27H, $C(CH_3)_3$), 1.78 (s, 6H, acac CH_3), 3.73 (s, 9H, OCH_3), 3.77 (s, 6H, NCH_2), 5.46 (s, 1H, acac CH), 6.51 (d, 3 Hz, 3H, ArH), 6.74 (d, 3 Hz, 3H, ArH). $^{13}C\{^1H\}$ NMR ($CDCl_3$): 26.32 (acac CH_3), 30.16 ($C(CH_3)_3$), 34.95 ($C(CH_3)_3$), 55.69 (NCH_2), 61.74 (OCH_3), 105.20 (acac CH), 111.56, 112.88, 125.66, 137.40, 151.81, 155.52, 190.30 (acac $C=O$). IR (evapd film, cm^{-1}): 2951 (m), 2909 (m), 2832 (w), 1739 (w), 1597 (m), 1520 (m), 1464 (s), 1428 (s), 1360 (m), 1320 (w), 1265 (m), 1239 (s), 1208 (s), 1142 (w), 1057 (m), 1025 (w), 979 (w), 919 (w), 837 (m), 795 (w), 767 (w), 665 (w). FAB-MS: 737 (M^+). UV-vis (CH_2Cl_2) λ_{max} 295 nm ($\epsilon = 25300 M^{-1} cm^{-1}$), 345 (13500), 384 (15400). Anal. Calcd for $C_{41}H_{55}NO_8Ti$: C, 66.75; H, 7.51; N, 1.90. Found: C, 66.87; H, 7.34; N, 1.87.

H,An_2N LTi(acac). In the drybox, 0.356 g of H,An_2N LTiH₃ (0.350 mmol) was added to a 25 mL round-bottom flask containing a Teflon-coated stir bar. The ligand was dissolved in CH_2Cl_2 , and 100 μ L of titanium isopropoxide (0.339 mmol, 0.97 equiv) was added via digital pipet. The flask was capped with a rubber septum, taken out of the drybox, and stirred for 5 min. Through the septum 2,4-pentanedione (35.0 μ L, 0.340 mmol, 0.97 equiv) was then added via syringe. After stirring under N_2 for 30 min, the flask was opened to the air and the solvent was removed on a rotary evaporator. The dark brown solid was crystallized by vapor diffusion of ether into a CH_2Cl_2 solution of the crude material to obtain 0.238 g of

H,An_2N LTi(acac) (60%). 1H NMR ($CDCl_3$): δ 1.97 (br s, 6H, acac CH_3), 3.70 (v br, 6H, NCH_2), 3.78 (s, 18H, OCH_3), 5.68 (s, 1H, acac CH), 6.46 (br d, 9 Hz, 3H, ArH H-3), 6.70 (d, 2.5 Hz, 3H, ArH H-6), 6.74 (d, 9 Hz, 12H, $NC_6H_4OCH_3$ 2,6-H), 6.79 (dd, 9, 2.5 Hz, 3H, ArH H-4), 6.93 (d, 9 Hz, 12H, $NC_6H_4OCH_3$ 3,5-H). $^{13}C\{^1H\}$ NMR ($CDCl_3$): 26.44 (acac CH_3), 55.69 (OCH_3), 61.50 (NCH_2), 105.47 (acac CH), 114.67, 116.55, 124.30, 124.42, 125.08, 125.78, 140.94, 142.16, 155.04, 157.65; acac CO too broad to be observed. IR (evapd film, cm^{-1}): 3038 (m), 2997 (m), 2950 (m), 2932 (m), 2906 (m), 2834 (s), 1585 (s), 1503 (s), 1485 (s), 1441 (s), 1362 (m), 1267 (s), 1241 (s), 1180 (m), 1148 (w), 1108 (m), 1036 (s), 931 (m), 887 (s), 825 (s), 808 (s), 780 (m), 735 (m), 703 (w), 683 (w), 770 (m), 639 (w), 598 (m). FAB-MS: 1160 (M^+). UV-vis (CH_2Cl_2) λ_{max} 302 nm ($\epsilon = 83400 M^{-1} cm^{-1}$), 358 (sh, 17900), 428 (17000). Anal. Calcd for $C_{68}H_{64}N_4O_{11}Ti$: C, 70.34; H, 5.56; N, 4.83. Found: C, 69.69; H, 5.64; N, 4.80.

tBu,An_2N LTi(acac). The compound was prepared analogously to tBu,MeO LTi(acac) using 0.2016 g of tBu,An_2N LTi(O'Bu) (0.1547 mmol) and 15.9 μ L of 2,4-pentanedione (0.155 mmol, 1.0 equiv) to yield 0.1837 g of tBu,An_2N LTi(acac) as a dark orange solid (91%). 1H NMR ($CDCl_3$): 1.24 (s, 27H, $C(CH_3)_3$), 1.93 (s, 6H, acac CH_3), 3.64 (s, 6H, NCH_2), 3.76 (s, 18H, OCH_3), 5.58 (s, 1H, acac CH), 6.55 (d, 2.5 Hz, 3H, ArH), 6.73 (d, 9 Hz, 12H, $NC_6H_4OCH_3$ 2,6-H), 6.88 (d, 2.5 Hz, 3H, ArH), 6.92 (d, 9 Hz, 12H, $NC_6H_4OCH_3$ 3,5-H). $^{13}C\{^1H\}$ NMR ($CDCl_3$): 26.18 (acac CH_3), 29.84 ($C(CH_3)_3$), 35.06 ($C(CH_3)_3$), 55.90 (OCH_3), 61.56 (NCH_2), 104.91 (acac CH), 114.57, 122.75, 122.86, 124.73, 126.08, 136.47, 139.60, 142.42, 154.75, 157.57, 190.30 (acac CO). IR (evapd film, cm^{-1}): 2998 (w), 2952 (m), 2907 (w), 2833 (w), 1655 (m), 1638 (m), 1596 (m), 1503 (s), 1464 (m), 1441 (m), 1360 (w), 1265 (w), 1239 (s), 1180 (m), 1141 (w), 1037 (m), 933 (w), 875 (m), 825 (m), 813 (m), 779 (w), 736 (w), 709 (w), 668 (w). FAB-MS: 1330 ($M+H$)⁺. UV-vis (CH_2Cl_2) λ_{max} 300 nm ($\epsilon = 80800 M^{-1} cm^{-1}$), 365 (sh, 13600), 432 (13300). Anal. Calcd for $C_{80}H_{88}N_4O_{11}Ti$: C, 72.28; H, 6.67; N, 4.21. Found: C, 71.60; H, 7.05; N, 3.86.

Electrochemistry. Electrochemical measurements were performed in the drybox using a BAS Epsilon potentiostat. A standard three-electrode setup was used, with a glassy carbon working electrode, Pt or glassy carbon counter electrode, and a silver/silver chloride pseudoreference electrode. The electrodes were connected to the potentiostat through electrical conduits in the drybox wall. Samples were approximately 1 mM in CH_2Cl_2 , using 0.1 M Bu_4NPF_6 as the electrolyte. Potentials were referenced to ferrocene/ferrocenium at 0 V,¹⁶ with the reference potential established by spiking the test solution with a small amount of ferrocene or decamethylferrocene ($E^\circ = -0.565$ V). Cyclic voltammograms were recorded with a scan rate of 60 mV s⁻¹. Square wave voltammograms were acquired with a step size of 3 mV, a pulse height of 30 mV, and a frequency of 15 Hz.

X-ray Crystallography of tBu,MeO LTiH₃, tBu,tBu LTiCl·0.5C₆H₆, and tBu,MeO LTiCl·C₆H₆. Very large crystals of tBu,MeO LTiH₃ deposited from a solution of the oily crude material from the preparation in methanol; a fragment was cut from a larger crystal for diffraction. Irregular orange crystals of tBu,tBu LTiCl·0.5C₆H₆ were grown by layering a solution in benzene with acetonitrile (1:5 v/v). Crystals of tBu,MeO LTiCl·C₆H₆ were grown by slow evaporation from benzene. All crystals were placed in inert oil before transferring to the cold N_2 stream of a Bruker Apex II CCD diffractometer. Data were reduced, correcting for absorption, using the program SADABS. The structures were solved using direct methods, except for tBu,MeO LTiCl·C₆H₆, which was solved using a Patterson synthesis. All nonhydrogen atoms not apparent from the initial solutions were found on difference Fourier maps, and all heavy atoms were refined anisotropically.

Table 1. Crystal Data for $t\text{Bu},\text{MeO}\text{LH}_3$, $t\text{Bu},t\text{Bu}\text{LTiCl}\cdot 0.5\text{C}_6\text{H}_6$, and $t\text{Bu},\text{MeO}\text{LTiCl}\cdot \text{C}_6\text{H}_6$

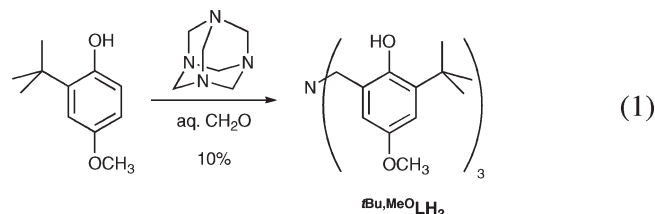
	$t\text{Bu},\text{MeO}\text{LH}_3$	$t\text{Bu},t\text{Bu}\text{LTiCl}\cdot 0.5\text{C}_6\text{H}_6$	$t\text{Bu},\text{MeO}\text{LTiCl}\cdot \text{C}_6\text{H}_6$
empirical formula	$\text{C}_{36}\text{H}_{51}\text{NO}_6$	$\text{C}_{48}\text{H}_{69}\text{ClNO}_3\text{Ti}$	$\text{C}_{42}\text{H}_{54}\text{ClNO}_6\text{Ti}$
temperature (K)	120(2)	100(2)	100(2)
λ	0.71073 (Mo K α)	0.71073 (Mo K α)	0.71073 (Mo K α)
space group	$P\bar{1}$	$P2_1/n$	$P2_12_12_1$
total data collected	28678	49294	47204
no. of indep reflns.	8436	11529	9703
R_{int}	0.0317	0.0308	0.0256
obsd. refls. [$I > 2\sigma(I)$]	6385	9394	9091
a (Å)	10.4142(8)	15.6030(8)	8.9631(4)
b (Å)	12.9974(10)	16.1332(8)	16.7443(6)
c (Å)	14.0615(10)	18.5363(9)	26.4720(10)
α (deg)	73.7099(11)	90	90
β (deg)	69.0650(11)	95.5600(10)	90
γ (deg)	88.2183(12)	90	90
V (Å ³)	1701.2(2)	4644.1(4)	3972.9(3)
Z	2	4	4
cryst size (mm)	$0.29 \times 0.26 \times 0.13$	$0.4 \times 0.3 \times 0.3$	$0.61 \times 0.35 \times 0.34$
no. refined params.	592	735	676
R indices [$I > 2\sigma(I)$] ^a	$R1 = 0.0392$, $wR2 = 0.0926$	$R1 = 0.0442$, $wR2 = 0.1173$	$R1 = 0.0272$, $wR2 = 0.0666$
R indices (all data) ^a	$R1 = 0.0559$, $wR2 = 0.1021$	$R1 = 0.0553$, $wR2 = 0.1262$	$R1 = 0.0307$, $wR2 = 0.0683$
goodness of fit	1.049	1.038	1.022

$$^a R1 = \sum ||F_o| - |F_c|| / \sum |F_o|; wR2 = [\sum w(F_o^2 - F_c^2)^2 / \sum w(F_o^2)]^{1/2}.$$

In the structure of $t\text{Bu},t\text{Bu}\text{LTiCl}\cdot 0.5\text{C}_6\text{H}_6$, two of the *tert*-butyl groups (those attached to C15 and C35) were disordered and were refined in two different orientations (the major orientations refined to 60.4(3)% and 57.6(3)% occupied, respectively). All hydrogens in the three structures, except those on the disordered *tert*-butyl groups and those on the lattice benzene in $t\text{Bu},t\text{Bu}\text{LTiCl}\cdot 0.5\text{C}_6\text{H}_6$, were found on difference Fourier maps and were refined isotropically. All calculations used SHELXTL (Bruker AXS),¹⁷ with scattering factors and anomalous dispersion terms taken from the literature.¹⁸ Further details about the individual structures are given in Table 1.

Results and Discussion

Preparation of Electron-Rich Tripodal Aminetris(phenol) Ligands. The most common method for preparing symmetrical aminetris(phenol) ligands $\text{N}(\text{CH}_2\text{C}_6\text{H}_2-3-\text{R}_1-5-\text{R}_2-2-\text{OH})_3$ is Mannich condensation of the appropriate 2,4-dialkylphenol with formaldehyde and ammonia.¹⁹ In this vein, reaction of 2-*tert*-butyl-4-methoxyphenol with hexamethylenetetramine and aqueous formaldehyde does give the tripodal ligand $\text{N}(\text{CH}_2\text{C}_6\text{H}_2-3-t\text{Bu}-5-\text{OMe}-2-\text{OH})_3$ ($t\text{Bu},\text{MeO}\text{LH}_3$) (eq 1). Yields are low, but the starting materials are inexpensive and the reaction can be run at a large scale, so this represents a simple route to prepare multigram quantities of the previously unknown methoxy-substituted ligand.



The free triphenol is revealed by X-ray crystallography (Tables 1–2) to have, at least in the solid state, an approximately C_3 -symmetric conformation with the three phenols pointed inward toward the lone pair of

Table 2. Selected Bond Distances (Å) and Angles (deg) in $t\text{Bu},\text{MeO}\text{LH}_3$

O1–C12	1.3754(14)
O2–C22	1.3806(13)
O3–C32	1.3849(13)
N–C10	1.4839(14)
N–C20	1.4804(13)
N–C30	1.4809(13)
C10–N–C20	111.26(8)
C10–N–C30	111.70(8)
C20–N–C30	108.66(8)
N–C10–C11	111.31(9)
N–C20–C21	111.56(9)
N–C30–C31	113.81(9)

the central nitrogen (Figure 2). This conformation, which is preorganized for metal binding, has been observed with other tripodal triphenols with *tert*-butyl groups in the *ortho* position,²⁰ while less bulky triphenols adopt a conformation with one of the OH groups turned away from the amine.²¹ A similar preorganized conformation has also been seen with other amine-centered tripodal ligands.²²

We then sought to make an even more electron-rich tripodal triphenol, with a diarylamino group in place of the *para*-methoxy group in $t\text{Bu},\text{MeO}\text{LH}_3$. Installation of the diarylamino group was envisaged to proceed via palladium-catalyzed amination of the appropriate (possibly protected) bromophenol, since this is known to be a highly efficient method for the formation of triarylamines.²³ Since literature precedent suggested that *p*-diarylamino phenols would be

(19) (a) Hultsch, K. *Chem. Ber.* **1949**, *82*, 16–25. (b) Dargaville, T. R.; De Bruyn, P. J.; Lim, A. S. C.; Looney, M. G.; Potter, A. C.; Solomon, D. H.; Zhang, X. *J. Polym. Sci. A: Polym. Chem.* **1997**, *35*, 1389–1398. (c) Cortes, S. A.; Hernández, M. A. M.; Nakai, H.; Castro-Rodríguez, I.; Meyer, K.; Fout, A. R.; Miller, D. L.; Huffman, J. C.; Mindiola, D. J. *Inorg. Chem. Commun.* **2005**, *8*, 903–907.

(20) Kelly, B. V.; Weintrob, E. C.; Buccella, D.; Tanski, J. M.; Parkin, G. *Inorg. Chem. Commun.* **2007**, *10*, 699–704.

(21) (a) Kubono, K.; Hirayama, N.; Kokusen, H.; Yokoi, K. *Anal. Sci.* **2001**, *17*, 913–914. (b) Chartres, J. D.; Dahir, A.; Tasker, P. A.; White, F. J. *Inorg. Chem. Commun.* **2007**, *10*, 1154–1158.

(22) Boon, J. M.; Lambert, T. N.; Smith, B. D.; Beatty, A. M.; Ugrinova, V.; Brown, S. N. *J. Org. Chem.* **2002**, *67*, 2168–2174.

(23) Hartwig, J. F. *Angew. Chem., Int. Ed.* **1998**, *37*, 2046–2067.

(17) Sheldrick, G. M. *Acta Crystallogr., Sect. A* **2008**, *A64*, 112–122.

(18) *International Tables for Crystallography*; Kluwer Academic Publishers: Dordrecht, The Netherlands, 1992; Vol. C.

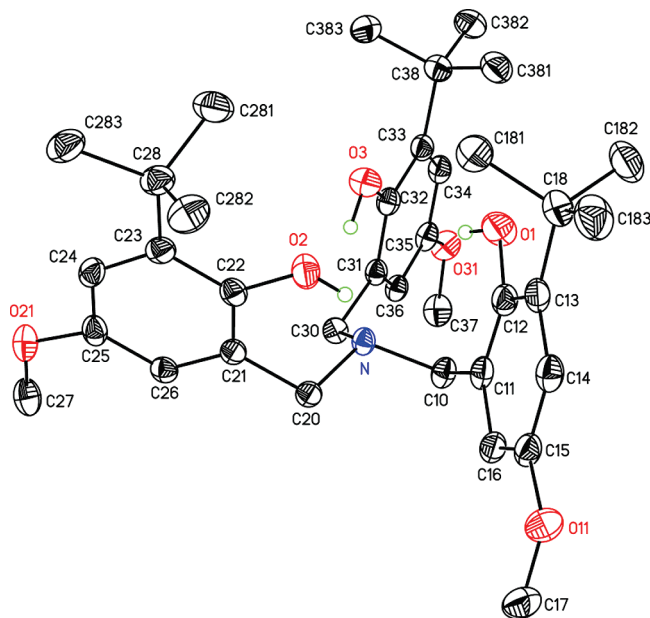
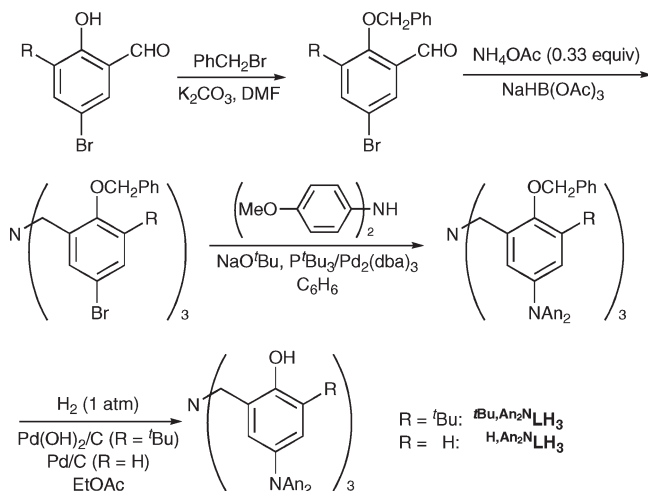


Figure 2. Thermal ellipsoid plot (50% ellipsoids) of $t\text{Bu,MeO-LH}_3$.

Scheme 1. Preparation of Diarylamino-Substituted Ligands $t\text{Bu,An}_2\text{N-LH}_3$ and $\text{H,An}_2\text{N-LH}_3$ (An = anisyl, $p\text{-C}_6\text{H}_4\text{OCH}_3$)



significantly air-sensitive,²⁴ we hoped to carry out the amination at a late stage of the synthesis. However, the appropriate phenolic starting material, 4-bromo-2-*tert*-butylphenol,²⁵ failed to undergo Mannich condensation with ammonia/formaldehyde, possibly because it is too electron-poor.

We thus turned to reductive amination to prepare a suitable aminotriphenol (Scheme 1), a strategy described by Licini.²⁶ Benzylation of 3-*tert*-butyl-5-bromo-2-hydroxybenzaldehyde (prepared by bromination of commercially available 3-*tert*-butylsalicylaldehyde¹⁴) proceeded smoothly and was followed by reductive amination using sodium triacetoxyborohydride in 1,2-dichloroethane²⁷ to give the

appropriate benzyl-protected brominated tribenzylamine. This was then subjected to $t\text{Bu}_3\text{P/Pd(0)}$ -catalyzed amination using 4,4'-dimethoxydiphenylamine in the presence of sodium *tert*-butoxide,²⁸ which provided the tris(triarylamine) in good yield. This material was somewhat light-sensitive and was stored in the dark before use.

Deprotection by hydrogenolysis using the standard catalyst, 10% palladium on carbon,^{26,29,30} was unsuccessful, with reactions even at elevated hydrogen pressures and high catalyst loadings proceeding at impractically slow rates. Attempted debenzylation using sodium iodide/trimethylsilyl chloride³¹ was also unsuccessful. However, Pearlman's catalyst (wet $\text{Pd(OH)}_2/\text{C}$) proved more active than Pd/C, and its use allowed hydrogenolysis to take place in high yield and in a reasonable amount of time. There was no sign of cleavage of the benzylic C–N bonds in these reactions, which contrasts sharply with reports that this catalyst (when used in ethanol) is actually selective for *N*-debzylolation in the presence of *O*-benzyl groups.³² The final deprotected ligand, $t\text{Bu,An}_2\text{N-LH}_3$, was moderately air-sensitive as a solid or in solution; it was decolorized with sodium dithionite after deprotection and then stored under nitrogen.

Unlike the Mannich condensation, which relies on blocking one of the positions *ortho* to the phenol to prevent polymer formation, the reductive amination sequence is compatible with a ligand that has no substituent *ortho* to the phenol. This ligand is prepared analogously (Scheme 1, R = H), starting with commercially available 5-bromosalicylaldehyde and proceeding through the previously prepared *O*-benzyl derivative.¹⁵ Debzylolation in the final step to yield the *ortho*-unsubstituted ligand $\text{H,An}_2\text{N-LH}_3$ proceeds smoothly with palladium on carbon as catalyst. Apparently either a *para*-diarylamino or an *ortho-tert*-butyl substituent by itself does not prevent hydrogenolysis over 10% Pd/C, but the combination of both renders the hydrogenolysis very sluggish with this catalyst.

Preparation and Characterization of Tripodal Titanium Complexes. The metalation of tripodal aminetriphenol ligands with titanium alkoxides is a general route to five-coordinate titanium alkoxides.^{10,11,29,30,33} The new *tert*-butyl substituted ligands $t\text{Bu,MeO-LH}_3$ and $t\text{Bu,An}_2\text{N-LH}_3$ both react with titanium(IV) *tert*-butoxide to give the corresponding $\text{LTi(O}^t\text{Bu)}$ complexes (Scheme 2). ^1H NMR spectroscopy at room temperature is consistent with C_3 -symmetry, with the appearance of the methylene hydrogens as a pair of doublets indicating a substantial barrier to racemization in the five-coordinate complex.¹⁰ As previously reported for $t\text{Bu,}^i\text{Bu-LTi}$ complexes,¹¹ the presence of the *ortho tert*-butyl substituents renders the

(28) Hartwig, J. F.; Kawatsura, M.; Hauck, S. I.; Shaughnessy, K. H.; Alcazar-Roman, L. M. *J. Org. Chem.* **1999**, *64*, 5575–5580.

(29) Axe, P.; Bull, S. D.; Davidson, M. G.; Gilfillan, C. J.; Jones, M. D.; Robinson, D. E. J. E.; Turner, L. E.; Mitchell, W. L. *Org. Lett.* **2007**, *9*, 223–226.

(30) Bernardinelli, G.; Seidel, T. M.; Kündig, E. P.; Prins, L. J.; Kolarovic, A.; Mba, M.; Pontini, M.; Licini, G. *Dalton Trans.* **2007**, 1573–1576.

(31) Olah, G. A.; Narang, S. C.; Gupta, B. G. B.; Malhotra, R. *J. Org. Chem.* **1979**, *44*, 1247–1251.

(32) (a) Marzi, M.; Misiti, D. *Tetrahedron Lett.* **1989**, *30*, 6075–6076. (b) Bernotas, R. C.; Cube, R. V. *Synth. Commun.* **1990**, *20*, 1209–1212.

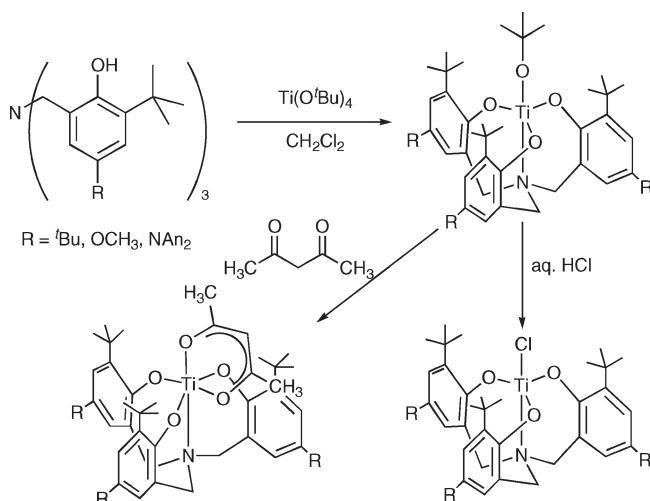
(33) (a) Kim, Y.; Verkade, J. G. *Organometallics* **2002**, *21*, 2395–2399. (b) Mba, M.; Prins, L. J.; Licini, G. *Org. Lett.* **2007**, *9*, 21–24.

(24) Linkletter, S. J. G.; Pearson, G. A.; Walter, R. I. *J. Am. Chem. Soc.* **1977**, *99*, 5269–5272.

(25) Berthelot, J.; Guette, C.; Desbene, P. L.; Basselier, J. J.; Chaquin, P.; Masure, D. *Can. J. Chem.* **1989**, *67*, 2061–2066.

(26) Prins, L. J.; Blázquez, M. M.; Kolarović, A.; Licini, G. *Tetrahedron Lett.* **2006**, *47*, 2735–2738.

(27) Abdel-Magid, A. F.; Carson, K. G.; Harris, B. D.; Maryanoff, C. A.; Shah, R. D. *J. Org. Chem.* **1996**, *61*, 3849–3862.

Scheme 2. Synthesis and Reactivity of ${}^t\text{Bu},\text{R}\text{LTi}$ Complexes ($\text{R} = {}^t\text{Bu}$, CH_3O , An_2N)

complexes resistant to hydrolysis, and both new *tert*-butoxide complexes can be handled in the air for moderate (${}^t\text{Bu},\text{An}_2\text{N}\text{LTi}(\text{O}^t\text{Bu})$) or extended (${}^t\text{Bu},\text{MeO}\text{LTi}(\text{O}^t\text{Bu})$) periods without degradation. The *ortho*-unsubstituted ligand $\text{H},\text{An}_2\text{N}\text{LH}_3$ reacts with $\text{Ti}(\text{O}^t\text{Bu})_4$ as well, but the product $\text{H},\text{An}_2\text{N}\text{LTi}(\text{O}^t\text{Bu})$ is quite moisture-sensitive and was not isolated. Tripods with small *ortho* substituents such as methyl³⁴ or phenyl³⁰ hydrolyze to give simple μ -oxo dimers, but hydrolysis of $\text{H},\text{An}_2\text{N}\text{LTi}(\text{O}^t\text{Bu})$ appears to be more complicated, with the compound reacting rapidly on exposure to air to give a mixture of products.

Apical group substitution in the *tert*-butyl compounds is straightforward, with the compounds reacting with aqueous HCl to provide the five-coordinate complexes LTiCl . The preparation of ${}^t\text{Bu},{}^t\text{Bu}\text{LTiCl}$ by reaction of ${}^t\text{Bu},{}^t\text{Bu}\text{LH}_3$ with TiCl_4 has been described by Nielson and co-workers,³⁴ and ${}^t\text{Bu},{}^t\text{Bu}\text{LTiCl}$ has similarly been prepared from $\text{TiCl}_4(\text{THF})_2$ and the corresponding free triphenol.^{19c} The coordination geometry of the compounds is confirmed by X-ray crystallography of both ${}^t\text{Bu},{}^t\text{Bu}\text{LTiCl}$ and ${}^t\text{Bu},\text{MeO}\text{LTiCl}$ (Figure 3, Tables 1 and 3), which crystallize as benzene solvates of isolated five-coordinate monomers. (${}^t\text{Bu},{}^t\text{Bu}\text{LTiCl}$ has also been crystallized as an etherate,³⁴ and data from this structure are included in Table 3 for comparison.) The three structures are extremely similar, with indistinguishable Ti–Cl and Ti–O distances, for example. The only hint that the *para*-methoxy group increases the electron-donating power of the aryloxides as expected is the slight elongation of the Ti–N distance in ${}^t\text{Bu},\text{MeO}\text{LTiCl}$ (0.036 Å and 0.056 Å longer than in the benzene and ether solvates, respectively, of ${}^t\text{Bu},{}^t\text{Bu}\text{LTiCl}$).

As reported previously for ${}^t\text{Bu},{}^t\text{Bu}\text{LTi}(\text{O}^t\text{Bu})$,¹² all of the *tert*-butoxide complexes ${}^t\text{Bu},\text{R}\text{LTi}(\text{O}^t\text{Bu})$ react quantitatively with 2,4-pentanedione to form the six-coordinate ${}^t\text{Bu},\text{R}\text{LTi}(\text{acac})$ complexes. The sterically unhindered complex $\text{H},\text{An}_2\text{N}\text{LTi}(\text{O}^t\text{Pr})$, generated in situ from $\text{H},\text{An}_2\text{N}\text{LH}_3$ and $\text{Ti}(\text{O}^t\text{Pr})_4$, reacts analogously to give air-stable $\text{H},\text{An}_2\text{N}\text{LTi}(\text{acac})$. While ${}^t\text{Bu},{}^t\text{Bu}\text{LTi}(\text{acac})$ is six-coordinate and has C_1 symmetry in the crystal, it (and all of the other

diketonate complexes) show room temperature NMR spectra with apparent C_{3v} symmetry of the tripod and equivalent ends of the acetylacetonate because of rapid fluxional processes.¹²

Optical spectra of the complexes (e.g., of $\text{LTi}(\text{acac})$, Figure 4) show intense ($\epsilon \sim 10^4 \text{ M}^{-1} \text{ cm}^{-1}$) absorptions in the near-UV and blue regions because of aryloxide-to-titanium charge transfer transitions.³⁵ Consistent with this assignment, changing the apical group on titanium from the more electron-donating *tert*-butoxide to the less electron-donating chloride results in a red shift of the absorption (for example, ${}^t\text{Bu},{}^t\text{Bu}\text{LTi}(\text{O}^t\text{Bu})$ is yellow, $\lambda_{\text{max}} = 329 \text{ nm}$, while ${}^t\text{Bu},{}^t\text{Bu}\text{LTiCl}$ is orange, $\lambda_{\text{max}} = 388 \text{ nm}$). The variation of λ_{max} with the *para* substituent on the aryloxide provides a gauge for the relative electron-donating power of the aryloxides (Table 4), with the peak charge-transfer absorption of ${}^t\text{Bu},{}^t\text{Bu}\text{LTi}(\text{acac})$ at 0.16 eV higher energy than that of ${}^t\text{Bu},\text{MeO}\text{LTi}(\text{acac})$, which is in turn blue-shifted 0.36 eV relative to ${}^t\text{Bu},\text{An}_2\text{N}\text{LTi}(\text{acac})$. The charge-transfer bands, especially those of ${}^t\text{Bu},{}^t\text{Bu}\text{LTi}(\text{acac})$ and ${}^t\text{Bu},\text{MeO}\text{LTi}(\text{acac})$, appear to have some shoulders on the high-energy side, possibly indicating the presence of overlapping bands of similar energy. This might result from slight differences between the aryloxide trans to the diketonate and those cis to it; in ${}^t\text{Bu},{}^t\text{Bu}\text{LTi}(\text{acac})$ the trans aryloxide forms a 0.038 Å shorter Ti–O bond than do the cis aryloxides.¹² The very intense peaks at about 300 nm and the less intense shoulders at about 360 nm in the diarylamino-substituted complexes are ligand-based transitions, as they correspond almost exactly to bands observed in $\text{N}(\text{C}_6\text{H}_4\text{OCH}_3)_3$.¹³

Electrochemistry of Tripodal Titanium Complexes.

Another way to gauge the relative electron-donating ability of the different tripodal complexes is through electrochemistry. The five-coordinate complexes $\text{LTi}(\text{O}^t\text{Bu})$ and LTiCl of the *tert*-butyl- and methoxy-substituted ligands show electrochemically irreversible voltammograms (Supporting Information, Figures S1–S2). One possible explanation for the observed irreversibility is that the coordinatively unsaturated species might bind electrolyte or aggregate in their oxidized forms. Consistent with this hypothesis, the six-coordinate acetylacetonate complexes all show well-defined, largely reversible oxidations in their cyclic voltammograms (Figure 5). Even the dialkyl-substituted complex ${}^t\text{Bu},{}^t\text{Bu}\text{LTi}(\text{acac})$ shows a single oxidation wave at $E^\circ = +0.57 \text{ V}$ (vs ferrocene/ferrocenium in dichloromethane), and the methoxy-substituted complex ${}^t\text{Bu},\text{MeO}\text{LTi}(\text{acac})$ shows two reversible oxidations, at $E^\circ = +0.33 \text{ V}$ and $+0.68 \text{ V}$ vs Fc^+/Fc . For comparison, the neutral six-coordinate d^0 tacn-tris(aryloxide) (Figure 1a) scandium complexes studied by Wiegardt et al. show first oxidations at $E^\circ = +0.52 \text{ V}$ and $+0.27 \text{ V}$ (measured in CH_3CN) for the *tert*-butyl and methoxy-substituted aryloxides, respectively.⁶ The similarity of the redox potentials of the scandium and titanium complexes supports the assignment of the oxidation as aryloxide-based (rather than, say, acac-centered) in the latter. The ~250 mV shift to lower potential on going from *tert*-butyl to methoxy has been observed consistently in a wide variety

(34) Nielson, A. J.; Shen, C.; Waters, J. M. *Polyhedron* **2006**, *25*, 2039–2054.

(35) (a) Tinoco, A. D.; Valentine, A. M. *J. Am. Chem. Soc.* **2005**, *127*, 11218–11219. (b) Tinoco, A. D.; Incarvito, C. D.; Valentine, A. M. *J. Am. Chem. Soc.* **2007**, *129*, 3444–3454.

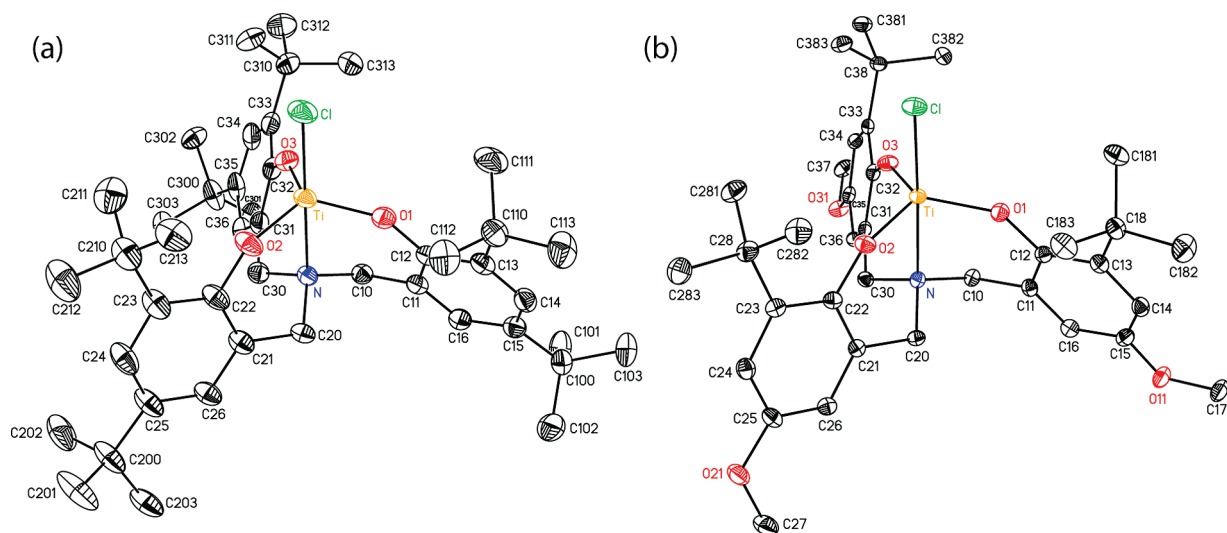


Figure 3. Thermal ellipsoid plots (50% ellipsoids) for (a) $t\text{Bu},r\text{BuLTiCl}\cdot 0.5\text{C}_6\text{H}_6$ and (b) $t\text{Bu,MeOLTiCl}\cdot\text{C}_6\text{H}_6$. Hydrogen atoms and solvents of crystallization are omitted for clarity.

Table 3. Selected Bond Distances (Å) and Angles (deg) in $t\text{Bu},r\text{BuLTiCl}\cdot 0.5\text{C}_6\text{H}_6$ and $t\text{Bu,MeOLTiCl}\cdot\text{C}_6\text{H}_6$ ^a

	$t\text{Bu},r\text{BuLTiCl}\cdot 0.5\text{C}_6\text{H}_6$	$t\text{Bu},r\text{BuLTiCl}\cdot \text{Et}_2\text{O}^{34}$	$t\text{Bu,MeOLTiCl}\cdot \text{C}_6\text{H}_6$
Ti–Cl	2.3130(4)	2.3074(7)	2.3118(4)
Ti–O1	1.8052(11)	1.809(2)	1.8132(10)
Ti–O2	1.8116(11)	1.817(2)	1.8126(9)
Ti–O3	1.8160(11)	1.811(2)	1.8031(9)
Ti–N	2.2361(11)	2.216(2)	2.2717(12)
N–Ti–Cl	179.87(4)	179.51(5)	177.98(3)
N–Ti–O1	83.04(4)	82.76(7)	83.26(4)
N–Ti–O2	83.45(4)	82.66(7)	82.61(4)
N–Ti–O3	82.15(4)	83.30(7)	81.94(4)
Cl–Ti–O1	96.99(3)	97.10(5)	98.17(3)
Cl–Ti–O2	96.65(4)	97.01(5)	95.46(3)
Cl–Ti–O3	97.73(4)	97.18(5)	98.53(3)
O1–Ti–O2	116.05(5)	119.29(7)	116.71(4)
O1–Ti–O3	117.65(5)	115.48(7)	119.76(4)
O2–Ti–O3	121.74(5)	120.72(7)	118.62(4)
Ti–O1–C12	144.16(9)	143.54(15)	143.36(9)
Ti–O2–C22	142.92(9)	143.66(14)	144.17(9)
Ti–O3–C32	144.91(10)	143.97(14)	146.47(9)

^a Corresponding data from $t\text{Bu},r\text{BuLTiCl}\cdot\text{Et}_2\text{O}$ (ref 34) are included for comparison.

of metal complexes.¹ The splitting between the first and second redox waves in $t\text{Bu,MeOLTi(acac)}$ is larger than that reported for its *tacn*-tris(aryloxy) scandium analogue (350 vs 200 mV), perhaps because of greater electrostatic effects in the lower dielectric solvent CH_2Cl_2 compared to CH_3CN .

The diarylamino-substituted complex $t\text{Bu,AN}_2\text{NLTi(acac)}$ shows two noteworthy differences from its *tert*-butyl and methoxy-substituted analogues. First, its initial oxidation takes place at a substantially lower potential ($\sim 0\text{ V}$ vs Fc^+/Fc). Second, while oxidation of the second arm of $t\text{Bu,MeOLTi(acac)}$ is 350 mV more difficult than oxidation of the first arm, all three aryloxides of $t\text{Bu,AN}_2\text{NLTi(acac)}$ lose an electron within about 200 mV of each other. While the three redox waves are very close in the cyclic voltammogram, they can be resolved in the square-wave voltammogram (Figure 6) at -0.09 , $+0.06$, and $+0.12\text{ V}$. There is a second set of three closely spaced waves in the CV and SWV between $+0.6$ and $+0.9\text{ V}$.

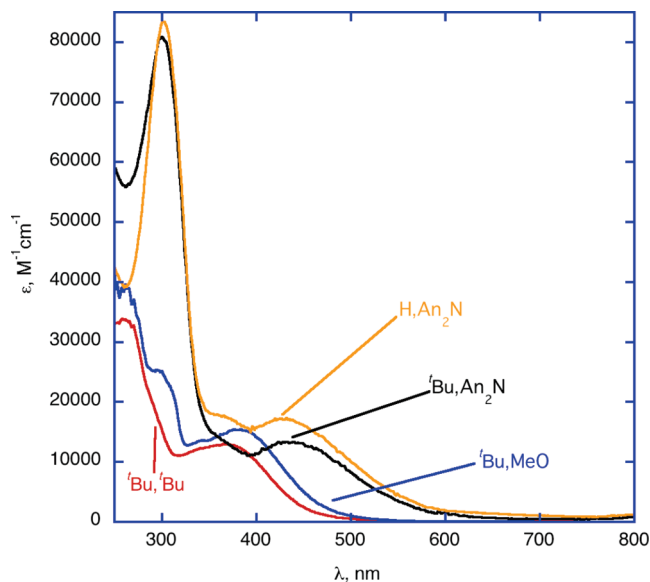


Figure 4. UV–visible spectra of LTi(acac) in CH_2Cl_2 .

Table 4. Optical and Electrochemical Properties of X,YLTi(acac)

X (ortho substituent)	Y (para substituent)	λ_{max} (LMCT)	E° , V vs $\text{Cp}_2\text{Fe}^+/\text{Cp}_2\text{Fe}$ (CH_2Cl_2 , 0.1 M $[\text{Bu}_4\text{N}]\text{PF}_6$)
$t\text{Bu}$	$t\text{Bu}$	366 nm (3.39 eV)	+0.57
$t\text{Bu}$	OMe	384 nm (3.23 eV)	+0.33, +0.68
$t\text{Bu}$	NAN_2	432 nm (2.87 eV)	−0.09, +0.06, +0.12, +0.58, +0.78, +0.90
H	NAN_2	428 nm (2.90 eV)	−0.02, +0.11, +0.16, +0.65, +0.84, +0.89

These are assigned to removal of a second electron from each of the dianisylaminophenoxide arms of the ligand. Such double oxidation of methoxy-substituted triarylamines has been documented to form diamagnetic quinonoid dicationic,³⁶ and the cyclic voltammetry of symmetrical $(\text{CH}_3\text{OC}_6\text{H}_4)_3\text{N}$ in CH_2Cl_2 shows reversible first and second oxidations at $+109$ and $+860\text{ mV}$ (vs Fc/Fc^+),

(36) Hagopian, L.; Köhler, G.; Walter, R. I. *J. Phys. Chem.* **1967**, *71*, 2290–2296.

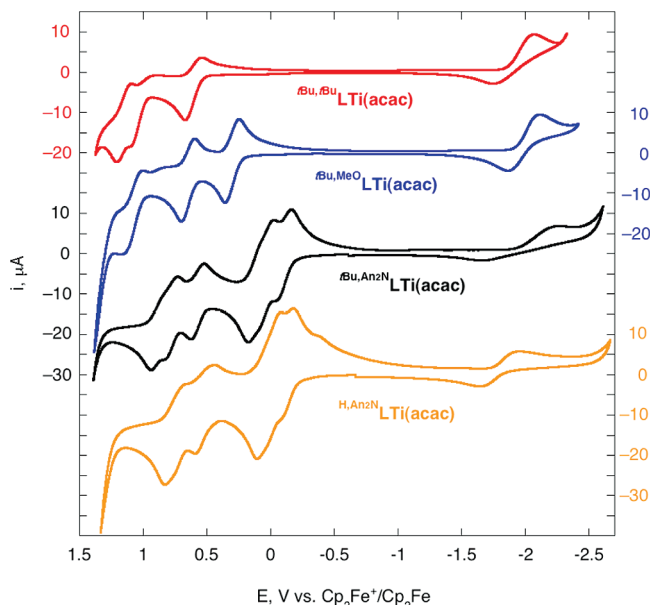


Figure 5. Cyclic voltammetry (CH_2Cl_2 , 0.1 M Bu_4NPF_6 , 60 mV/s) of 1 mM solutions of (from top to bottom) ${}^t\text{Bu}, {}^t\text{BuLTi}(\text{acac})$, ${}^t\text{Bu}, \text{MeOLTi}(\text{acac})$, ${}^t\text{Bu}, \text{An}_2\text{NLTi}(\text{acac})$, and $\text{H}, \text{An}_2\text{NLTi}(\text{acac})$.

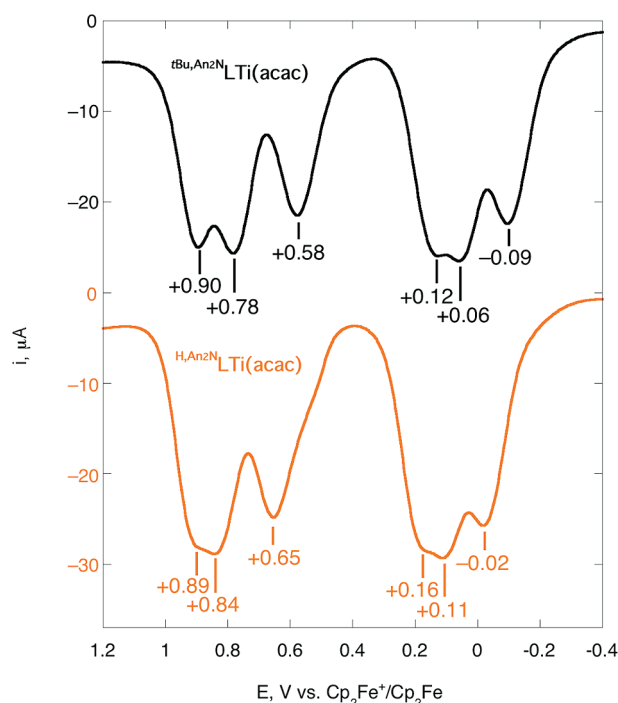


Figure 6. Square wave voltammetry (CH_2Cl_2 , 0.1 M $(\text{Bu}_4\text{N})\text{PF}_6$) of ${}^t\text{Bu}, \text{An}_2\text{NLTi}(\text{acac})$ (top) and $\text{H}, \text{An}_2\text{NLTi}(\text{acac})$ (bottom).

respectively.¹³ We have prepared the unsymmetrical dimethoxytriarylamine $(\text{CH}_3\text{OC}_6\text{H}_4)_2\text{NC}_6\text{H}_4\text{COCH}_3$ (see Supporting Information for details of preparation and characterization), and find that it also shows two reversible oxidations in its CV, shifted as expected to higher potential because of the replacement of one methoxy group by an acetyl group (Supporting Information, Figure S3, $E^\circ = +0.38$, $+1.03$ V). The 650–750 mV difference between the first and second oxidations in these triarylamines compares favorably to the 670–780 mV shifts seen in ${}^t\text{Bu}, \text{An}_2\text{NLTi}(\text{acac})$ and strongly supports the proposed assignments.

The electrochemistry of the *ortho*-unsubstituted $\text{H}, \text{An}_2\text{NLTi}(\text{acac})$ is strikingly similar to that of the more hindered ${}^t\text{Bu}, \text{An}_2\text{NLTi}(\text{acac})$ (Figures 5–6), except for a shift of the redox potentials by about +50 mV, consistent with the *tert*-butyl group being slightly more electron-donating than hydrogen. Notably, the reversibility of the electrochemical redox reactions remains excellent even in the absence of steric protection of the phenoxide center. This contrasts with the results of oxidation of the tacntris(dialkylphenoxide) complexes, where the dimethylphenoxides show irreversible electrochemistry, while the di-*tert*-butylphenoxides can be oxidized reversibly.⁶

Qualitatively, the ~400 mV shift to lower potential in ${}^t\text{Bu}, \text{An}_2\text{NLTi}(\text{acac})$ compared to ${}^t\text{Bu}, \text{MeOLTi}(\text{acac})$ is expected, given the greater donating ability of amino compared to alkoxy substituents.³⁷ For example, a dimethylamino-substituted salen nickel complex has been observed to undergo ligand-centered oxidation at 400 mV lower potential than its methoxy-substituted analogue.³⁸ A second explanation for the lower redox potentials is that the locus of oxidation shifts, at least in part, to the diarylamino groups in $\text{R}, \text{An}_2\text{NLTi}(\text{acac})$. Consistent with this view is the similarity in redox potentials between $(\text{CH}_3\text{OC}_6\text{H}_4)_3\text{N}$ ($E^\circ = +0.11$ V)¹³ and $\text{R}, \text{An}_2\text{NLTi}(\text{acac})$ ($E^\circ = -0.09$ and -0.02 V for $\text{R} = {}^t\text{Bu}$ and $\text{R} = \text{H}$, respectively). Analysis of a series of *p*-substituted radical cations $(\text{XC}_6\text{H}_4)_3\text{N}^{+\bullet}$ by EPR indicates that ^{14}N and *ortho*- ^1H hyperfine constants are fairly constant for $\text{X} = \text{alkyl}$, H , or electron-withdrawing substituents, but are modestly ($\text{X} = \text{OCH}_3$) or substantially ($\text{X} = \text{NH}_2$) reduced for electron-donating substituents,³⁹ suggesting partial delocalization of the radical onto these substituents. Combined with the electrochemical results, this suggests that oxidation occurs principally from the diarylamino groups in $\text{R}, \text{An}_2\text{NLTi}(\text{acac})$, but with significant interactions with the aryloxy group. This view is also consistent with the small, but detectable, electrochemical splittings in the first and second oxidation waves. The fact that the splittings between the oxidation potential of the three arms are small ($\Delta E^\circ = 50$ – 150 mV) suggests that the loci of oxidation are relatively far from each other and so there is little sensitivity of the redox potential to partial oxidation of the ligand. This contrasts with the much larger splitting between waves seen in the more aryloxy-localized ${}^t\text{Bu}, \text{MeOLTi}(\text{acac})$ ($\Delta E^\circ = 350$ mV). However, the fact that there is any discernible splitting at all indicates that the oxidation of one arm has some effect on the electron density at the other arms. In contrast, a recent study of bis(ferrocenyldiketonate) complexes of titanium(IV), where DFT calculations showed the redox-active orbitals to be essentially localized on iron, showed no discernible splitting in the ferrocene-based redox waves.⁴⁰ Both the narrow spread of oxidation potentials (to minimize overpotentials), and the existence of some coupling (as an indication of interactions with the metal center), validate the ligand

(37) Hansch, C.; Leo, A.; Taft, R. W. *Chem. Rev.* **1991**, *91*, 165–195.

(38) Rotthaus, O.; Jarjayes, O.; Del Valle, C. P.; Philouze, C.; Thomas, F. *Chem. Commun.* **2007**, 4462–4464.

(39) Pearson, G. A.; Rocek, M.; Walter, R. I. *J. Phys. Chem.* **1978**, *82*, 1185–1192.

(40) Dulatas, L. T.; Brown, S. N.; Ojomo, E.; Noll, B. C.; Cavo, M. J.; Holt, P. B.; Wopperer, M. M. *Inorg. Chem.* **2009**, *48*, 10789–10799.

design of the (diarylamino)aryloxides as promising candidates for supporting redox reactions.

Conclusions

Electron-rich tripodal aminetriaryloxide ligands can be prepared by Mannich condensation (${}^{t\text{Bu},\text{MeO}}\text{LH}_3$) or by a synthetic sequence involving reductive amination of a protected bromosalicylaldehyde and Hartwig–Buchwald amination as key steps (${}^{t\text{Bu},\text{Ar}_2\text{N}}\text{LH}_3$ and ${}^{\text{H},\text{Ar}_2\text{N}}\text{LH}_3$). Both five-coordinate (${}^{t\text{Bu},\text{X}}\text{LTi}(\text{O}^t\text{Bu})$ and ${}^{t\text{Bu},\text{X}}\text{LTiCl}$) and six-coordinate ($\text{LTi}(\text{acac})$) complexes of titanium(IV) can be prepared. Electrochemistry of the diarylamino-substituted tripods shows that each can be reversibly oxidized by up to six electrons (two per arm). As possible redox reservoirs for reactions where substrate oxidation is mediated by a redox-inert metal, the diarylamino-substituted tripods display three critical features: (1) They support low coordination numbers, potentially allowing substrate access to the metal center. (2) The redox potentials for oxidation of successive arms are closely spaced ($\Delta E^\circ = 50\text{--}150\text{ mV}$), reducing the possibility of large overpotentials. (3) The redox potentials for oxidation of successive arms do show some variation, indicating that there is modest interaction between the redox centers and the metal center, opening the possibility of communicating the redox state of the ligand to a substrate bound to the metal.

The translation of this potential into actual reactivity is currently being explored.

Acknowledgment. We thank Dr. Allen G. Oliver for his assistance with the crystal structure of ${}^{t\text{Bu},\text{MeO}}\text{LH}_3$, Dr. Alicia M. Beatty for her assistance with the crystal structure of ${}^{t\text{Bu},t\text{Bu}}\text{LTiCl}\cdot 0.5\text{ C}_6\text{H}_6$, and Ms. Nancy E. Roback for her assistance with the crystal structure of $(\text{MeOC}_6\text{H}_4)_2\text{NC}_6\text{H}_4\text{COCH}_3$. This work was supported by the donors of the Petroleum Research Fund, administered by the American Chemical Society, and by the National Science Foundation (CHE-0518243). D.L. gratefully acknowledges the Notre Dame College of Science for a summer undergraduate research fellowship, and A.J.M. thanks the Notre Dame College of Science and the Glynn Family Honors Program for summer fellowship support. Partial support for the X-ray diffraction facility was provided by the NSF (CHE-0443233).

Supporting Information Available: Crystallographic information on ${}^{t\text{Bu},\text{MeO}}\text{LH}_3$, ${}^{t\text{Bu},t\text{Bu}}\text{LTiCl}\cdot 0.5\text{ C}_6\text{H}_6$, ${}^{t\text{Bu},\text{MeO}}\text{LTiCl}\cdot \text{C}_6\text{H}_6$, and $(\text{MeOC}_6\text{H}_4)_2\text{NC}_6\text{H}_4\text{COCH}_3$ in CIF format; cyclic voltammetry of $\text{LTi}(\text{O}^t\text{Bu})$ and LTiCl and synthetic details and spectroscopic, structural, and electrochemical characterization of $(\text{MeOC}_6\text{H}_4)_2\text{NC}_6\text{H}_4\text{COCH}_3$ (PDF format). This material is available free of charge via the Internet at <http://pubs.acs.org>.